



This discussion paper is/has been under review for the journal Atmospheric Chemistry and Physics (ACP). Please refer to the corresponding final paper in ACP if available.

# Observations and modeling of air quality trends over 1990–2010 across the Northern Hemisphere: China, the United States and Europe

J. Xing<sup>1</sup>, R. Mathur<sup>1</sup>, J. Pleim<sup>1</sup>, C. Hogrefe<sup>1</sup>, C.-M. Gan<sup>1</sup>, D. C. Wong<sup>1</sup>, C. Wei<sup>1,2</sup>, R. Gilliam<sup>1</sup>, and G. Pouliot<sup>1</sup>

<sup>1</sup>The US Environmental Protection Agency, Research Triangle Park, NC 27711, Durham, USA  
<sup>2</sup>Multiphase Chemistry Department, Max Planck Institute for Chemistry, 55128 Mainz, Germany

Received: 22 August 2014 – Accepted: 18 September 2014 – Published: 8 October 2014

Correspondence to: J. Xing (xing.jia@epa.gov)

Published by Copernicus Publications on behalf of the European Geosciences Union.

Observations and modeling of air quality trends over 1990–2010 across the Northern Hemisphere

J. Xing et al.

Title Page

Abstract

Introduction

Conclusions

References

Tables

Figures



Back

Close

Full Screen / Esc

Printer-friendly Version

Interactive Discussion



## Abstract

Trends in air quality across the Northern Hemisphere over a 21 year period (1990–2010) were simulated using the CMAQ multiscale chemical transport model driven by meteorology from WRF simulations and internally consistent historical emission inventories obtained from EDGAR. Thorough comparison with several ground observation networks mostly over Europe and North America was conducted to evaluate the model performance as well as the ability of CMAQ to reproduce the observed trends in air quality over the past two decades in three regions: eastern China, the continental United States and Europe.

The model successfully reproduced the observed decreasing trends in SO<sub>2</sub>, NO<sub>2</sub>, maxima 8 h O<sub>3</sub>, SO<sub>4</sub><sup>2-</sup> and EC in the US and Europe. However, the model fails to reproduce the decreasing trends in NO<sub>3</sub><sup>-</sup> in the US, potentially pointing to uncertainties of NH<sub>3</sub> emissions. The model failed to capture the 6 year trends of SO<sub>2</sub> and NO<sub>2</sub> in CN-API from 2005–2010, but reproduced the observed pattern of O<sub>3</sub> trends shown in three WDCGG sites over eastern Asia. Due to the coarse spatial resolution employed in these calculations, predicted SO<sub>2</sub> and NO<sub>2</sub> concentrations are underestimated relative to all urban networks, i.e., US-AQS (NMB = -46 and -54 %), EU-AIRBASE (NMB = -12 and -57 %) and CN-API (NMB = -36 and -68 %). Conversely, at the rural network EU-EMEP SO<sub>2</sub> is overestimated (NMB from 4 to 150 %) while NO<sub>2</sub> is simulated well (NMB within ±15 %) in all seasons. Correlations between simulated and observed winter time daily maxima 8 h (DM8) O<sub>3</sub> are poor compared to other seasons for all networks. Better correlation between simulated and observed SO<sub>4</sub><sup>2-</sup> was found compared to that for SO<sub>2</sub>. Underestimation of summer SO<sub>4</sub><sup>2-</sup> in the US may be associated with the uncertainty in precipitation and associated wet scavenging representation in the model. The model exhibits worse performance for NO<sub>3</sub><sup>-</sup> predictions, particularly in summer, due to high uncertainties in the gas/particle partitioning of NO<sub>3</sub><sup>-</sup> as well as seasonal variations of NH<sub>3</sub> emissions. There are high correlations (*R* > 0.5) between observed and simulated EC, although the model underestimates the

## Observations and modeling of air quality trends over 1990–2010 across the Northern Hemisphere

J. Xing et al.

Title Page

Abstract

Introduction

Conclusions

References

Tables

Figures

◀

▶

◀

▶

Back

Close

Full Screen / Esc

Printer-friendly Version

Interactive Discussion



EC concentration by 65 % due to the coarse grid resolution as well as uncertainties in the PM speciation profile associated with EC emissions.

The almost linear response seen in the trajectory of modeled  $O_3$  changes in the eastern China over the past two decades, suggests that control strategies that focus on combined control of  $NO_x$  and VOC emissions with a ratio of 0.46 may provide the most effective means for  $O_3$  reductions for the region devoid of non-linear response potentially associated with  $NO_x$  or VOC limitation resulting from alternate strategies. The response of  $O_3$  is more sensitive to changes in  $NO_x$  emissions in the eastern US because the relative abundance of biogenic VOC emissions tends to reduce the effectiveness of VOC controls. Increasing  $NH_3$  levels offset the relative effectiveness of  $NO_x$  controls in reducing the relative fraction of aerosol  $NO_3^-$  formed from declining  $NO_x$  emissions in the eastern US, while the control effectiveness was assured by the simultaneous control of  $NH_3$  emission in Europe.

## 1 Introduction

The last two decades have witnessed significant changes in air pollutant emissions across the globe. Developed countries in North America and Europe have implemented emission reduction measures which have led to a continuous improvement in air quality. Conversely, in developing regions of the world, in Asia in particular, though control actions have been taken, their effectiveness has been overwhelmed by the sharp increase in emissions resulting from increased energy demand associated with rapidly growing economies and populations. The striking contrast in the trends in air quality between developed and developing countries has been well discussed in recent years (e.g., Richter et al., 2005). It is also believed that the observed “dimming” and “brightening” trends over the past two decades is primarily related to the changes of emission patterns over Northern Hemisphere (e.g., Wild, 2009; Gan et al., 2014). Therefore, an accurate description of the decadal variations in emissions and associated aerosol burden in the atmosphere is the basis of any attempts to explain the causes of decadal

### Observations and modeling of air quality trends over 1990–2010 across the Northern Hemisphere

J. Xing et al.

Title Page

Abstract

Introduction

Conclusions

References

Tables

Figures



Back

Close

Full Screen / Esc

Printer-friendly Version

Interactive Discussion



changes in surface solar radiations and short-term climate forcing issues arising from human activities.

Improving air quality and protecting the health and welfare of their people is the ultimate goal for any country. Studies on historical trends in air quality can provide an indication of progress in the direction as well as an assessment of future steps towards the goal. On the basis of long-term records, the effectiveness of past or current control policy can be evaluated and suitable control strategies can be designed for the future. In Europe and North America, several monitoring networks have been in operation for decades and observational records available at some networks are long enough to be used in trends analysis studies (e.g., Sickles and Shadwick, 2007). Such records are vital not only because they reflect the changes in air quality over time, but also because they can be used to evaluate long-term trends in air quality arising from estimated changes in historical emissions, simulated by air quality models. Colette et al. (2011) analyzed the air quality trends during 1998–2007 over Europe by using observations of European Monitoring and Evaluation Programme (EU-EMEP, <http://www.emep.int>) and the European Air quality data Base (EU-AIRBASE, <http://acm.eionet.europa.eu/databases/airbase/>) records as well as model simulations. Hogrefe et al. (2009) adjusted six-year model simulations (2000–2005) by using the observed  $PM_{2.5}$  species concentrations from the observations of Interagency Monitoring of Protected Visual Environments (US-IMPROVE, <http://vista.cira.colostate.edu/improve/>) and Chemical Speciation Network (CSN) sites in the northeastern US. Trends in  $O_3$  concentration and  $SO_4^{2-}$ ,  $NO_3^-$  depositions from 1988–2005 simulated by the same model were also compared with long term observations (Civerolo et al., 2010; Hogrefe et al., 2011). However, due to the large computational cost, very few studies have examined in decadal trend in air pollution over large regions such as Northern Hemisphere. Koumoutsaris and Bey (2012) evaluated the global model performance of  $O_3$  trends simulation (1991–2005) through comparison with long-term observed records from EMEP, the World Data Centre for Greenhouse Gases (WDCGG, <http://ds.data.jma.go.jp/gmd/wdcgg/>) and the Clean Air Status and Trends Network (US-CASTNET, <http://epa.gov/castnet/>).

**Observations and modeling of air quality trends over 1990–2010 across the Northern Hemisphere**

J. Xing et al.

Title Page

Abstract

Introduction

Conclusions

References

Tables

Figures



Back

Close

Full Screen / Esc

Printer-friendly Version

Interactive Discussion



## Observations and modeling of air quality trends over 1990–2010 across the Northern Hemisphere

J. Xing et al.

Title Page

Abstract

Introduction

Conclusions

References

Tables

Figures

◀

▶

◀

▶

Back

Close

Full Screen / Esc

Printer-friendly Version

Interactive Discussion

Long-term records of lower troposphere O<sub>3</sub> concentrations from selected sites which are believed to represent baseline conditions in Europe (Logan et al., 2012) and the US (Parrish et al., 2009, 2012) were used to make quantitative comparisons of simulation results from three chemistry-climate models (NCAR CAM-chem, GFDL-CM3, and GISS-E2-R) (Parrish et al., 2014). To date however limited attempts have been made to systematically assess long-term trends in multiple linked atmospheric pollutants (ox-

idants, particles and acidifying substances) across regional to hemispheric scales. As a regional chemistry transport model (CTM), the Community Multiscale Air Quality (CMAQ) modeling (version 5.0) system (Binkowski and Roselle, 2003; Byun and Schere, 2006; Foley et al., 2010) has previously been successfully applied for several quality studies over North America (Eder and Yu, 2006; Appel et al., 2007, 2008; Mathur et al., 2008), Europe (Matthias et al., 2012; Kukkonen et al., 2012) and eastern Asia (Yamaji et al., 2006; Wang et al., 2011a; Xing et al., 2011a). However, the need for time varying lateral boundary conditions (LBCs) which are usually derived from global CTMs simulations limits its applications in trend analysis over decades. Recently, the applicability of CMAQ model has been successfully extended to hemispheric scales (Mathur et al., 2012, 2014), so that the application of hemispheric CMAQ provides a consistent approach to generate LBCs for nested regional domains employing finer resolution.

Changing emission patterns across the globe over the past two decades have influenced background air pollution levels for different regions across the Northern Hemisphere. To examine air quality trends in different regions over Northern Hemisphere, we used a multiscale chemical transport model (i.e., CMAQ) driven by historical emission inventories and meteorological dataset to simulate air quality from 1990–2010. The ability of the multiscale model to reproduce observed trends over the Northern Hemisphere, including North America, Europe and East Asia, was assessed. A brief description of the model configuration, emission processing and observations is given in Sect. 2. The evaluation of model performance through comparison with long-term



## Observations and modeling of air quality trends over 1990–2010 across the Northern Hemisphere

J. Xing et al.

Title Page

Abstract

Introduction

Conclusions

References

Tables

Figures

◀

▶

◀

▶

Back

Close

Full Screen / Esc

Printer-friendly Version

Interactive Discussion



Atmospheric Research, version 4.2) (European Commission, 2011) provides a consistent global emission inventories for 1970–2008 for 17 anthropogenic sectors on a  $0.1^\circ \times 0.1^\circ$  resolution. In this study, we used year specific EDGAR emission for the period 1990–2008. Estimates for 2009 and 2010 were derived from projections based on three most recent references for the United States (Xing et al., 2013), Europe (EEA, 2012) and China (He, 2012). In Europe and North America, pollutant emissions,  $\text{SO}_2$  and  $\text{NO}_x$  in particular, have seen continuous reductions during 1990–2010 (refer to Fig. 2). In contrast,  $\text{NO}_x$  and VOC emissions in China have continuously increased, while  $\text{SO}_2$  increased during 1990–2006 then decreased from 2007 to 2010 due to more recent strict controls (Zhao et al., 2013; Wang et al., 2014). Emissions in other areas during 2009–2010 were kept the same as the 2008 values. Additionally, since EDGARv4.2 provides only  $\text{PM}_{10}$  emissions,  $\text{PM}_{2.5}$  emissions were estimated by deriving the ratio of  $\text{PM}_{2.5}$  to  $\text{PM}_{10}$  from the 2000–2005 EDGAR HTAP (Hemispheric Transport of Air Pollution, version 1) inventory (Janssens-Maenhout et al., 2012) which provides both  $\text{PM}_{10}$  and  $\text{PM}_{2.5}$  emissions and then applying this ratio to split EDGARv4.2  $\text{PM}_{10}$  emissions into  $\text{PM}_{2.5}$  and  $\text{PM}_{2.5-10}$ . Biogenic VOC and lightning  $\text{NO}_x$  emissions were obtained from GEIA (Global Emission Inventory Activity) (Guenther et al., 1995; Price et al., 1997) and were kept the same for all years during 1990–2010. The  $0.1^\circ$  resolution gridded data was spatially allocated to the CMAQ grid ensuring conservation of mass. Vertical profiles for anthropogenic sectors and lightning were based on Simpson et al. (2003) and Ott et al. (2010), respectively. The annual mean emissions in each sector were distributed into each hour for each simulated day using the EDGAR default temporal profiles which are primarily based on some western European data (<http://themasites.pbl.nl/tridion/en/themasites/edgar/documentation/content/Temporal-variation.html>). Emissions of  $\text{PM}_{2.5}$  and NMVOC were further speciated into AERO6 and CB05 species based on default profiles in Sparse Matrix Operator Kernel Emissions modeling system (SMOKE, <http://cmasceneter.org/smoke/>) which is primarily based on data for the United States. Uncertainties are expected when region specific temporal and speciation profiles are applied to all other counties; however this approach is reasonable

given the lack of any additional information. Further improvement and data are needed to develop more representative profiles for other countries.

### 2.3 Observed long-term trends

Table 1 summarizes the dataset used in this study, which includes three networks in the United States, i.e., Air Quality System, (US-AQS, <http://www.epa.gov/ttn/airs/airsaqs/>), US-CASTNET and US-IMPROVE; two networks in Europe, i.e., EU-EMEP and EU-AIRBASE; one in China (CN-API, Air Pollution Index) and one global network (WD-CGG). Among these, records of US-CASTNET, US-IMPROVE and EU-EMEP are specifically designed for trend assessments since most of their sites are located in rural background areas to represent regional atmospheric pollution. Sites in US-AQS and EU-AIRBASE are typically closer to urban areas and may be impacted by local pollution and features sub-grid to the model resolution. CN-API is the average of observed air pollutant concentrations from urban monitoring sites in each city and represents records in 7 Chinese cities (i.e., Beijing, Shanghai, Guangzhou, Xi'an, Wuhan, Guiyang, Guilin) (Jiang et al., 2004; Wang et al., 2011a). In addition, 3 selected WD-CGG sites were used for O<sub>3</sub> trends analysis in East Asia. Only data at sites that covered the 75% of entire 21 year period (i.e., at least 18 available years with > 75% coverage for each year) is considered except in the case of CN-API which was only recently set up in early 2000s and in the case of US-CASTNET (for O<sub>3</sub> only) because most sites have no O<sub>3</sub> records in winter (criteria set as at least 15 available years with > 75% coverage from March to November for each year). Details about the time-period covered, the number of sites selected for analysis as well as the record frequency for each network can be found in Table 1. Model results at each monitor location were matched in time to the available record; thus model data was not considered during period of missing observations, in either the statistical evaluation or in the trend analysis.

To evaluate the model's performance, model-observed comparisons were conducted by network and pollutant. Five statistical measures: correlation coefficient ( $R$ ), Mean Bias (MB), Normalized Mean Bias (NMB), Root Mean Squared Error (RMSE) and

## Observations and modeling of air quality trends over 1990–2010 across the Northern Hemisphere

J. Xing et al.

Title Page

Abstract

Introduction

Conclusions

References

Tables

Figures

◀

▶

◀

▶

Back

Close

Full Screen / Esc

Printer-friendly Version

Interactive Discussion



Normalized Mean Error (NME) are employed for evaluation. In consideration of the limited length of record, this study only focuses on linear trends (Colette et al., 2011). The linear least square fit method was employed and significance of trends was examined with a Student  $t$  test at the 95 % confidence level ( $p = 0.05$ ).

## 3 Result

### 3.1 Model performance

Table 2 summaries the statistics of model performance for gaseous species (Table 2a) and fine particles (Table 2b).

#### 3.1.1 SO<sub>2</sub> and NO<sub>2</sub> concentration

Model performance characteristics for SO<sub>2</sub>, primarily emitted from point sources, can largely be attributed to artificial dilution effects over the large grid volumes employed here. As expected, a hemispherical simulation with relatively coarse spatial resolution is unable to accurately capture the peak values. As seen in Table 2a, SO<sub>2</sub> is underestimated for all urban networks characterized by higher concentrations than rural network, i.e., US-AQS underestimated by 46 %, EU-AIRBASE by 12 % and CN-API by 36 %. For rural network EU-EMEP, SO<sub>2</sub> is overestimated in all seasons (4–150 %). A small bias is evident for US-CASTNET annual concentrations since the overestimation in fall is compensated by the underestimation in spring and winter.

Similar performance is noted for simulated NO<sub>2</sub>. The model significantly underestimates NO<sub>2</sub> at urban networks: US-AQS by 54 %, EU-AIRBASE by 57 % and CN-API by 68 %. However, much better performance is noted at sites in the rural network EU-EMEP with bias within  $\pm 15$  % in all seasons. Though the model-observation correlation coefficients ( $R$ ) are low for EU-AIRBASE (0.18) and CN-API (0.08) on annual basis, the MB in EU-AIRBASE ( $-17.7 \mu\text{g m}^{-3}$ ) is comparable with previous modeling as reported by Colette et al. (2011) ( $-6.5$  to  $-18.1 \mu\text{g m}^{-3}$ ) and the magnitude of NMB in CN-API

(67.5%) is comparable with Wang et al. (2009) (−61.2 to −81.3%) but in opposite direction. It is expected that the performance should be better when simulations are conducted with finer horizontal resolution and with more accurate spatially-resolved emissions.

### 3.1.2 O<sub>3</sub> concentration

Model performance for O<sub>3</sub> is examined through comparisons of seasonal or annual maxima of the daily maxima 8 h (DM8) average or 1 h values since those are the metrics most relevant to air quality standards and health assessments.

Correlation coefficients in EU-AIRBASE (0.4) are lower than Colette et al. (2011) (0.6–0.8) because the frequency of the observed record used in this study is annual, and therefore, the correlation coefficients calculated here do not benefit from the fact that the model simulations generally capture the observed seasonal cycle. However, the MB (14.4 μg m<sup>−3</sup>) is comparable with that reported in Colette et al. (2011) (−4.3 to 18.5 μg m<sup>−3</sup>). Simulations in winter ( $R = 0.3$ – $0.5$ ) have the worse correlation with observations for all networks compared to those in other seasons ( $R = 0.6$ – $0.8$ ). On the other hand, both NMB (−13.6 to 16.9%) and NME (< 25.9%) are fairly small in all seasons and comparable with that reported by Zhang et al. (2009) (NMB: −10.6 to 15.9%; NME: < 25.4%) and Wang et al. (2009) (|NMB| < 37.9%).

### 3.1.3 SO<sub>4</sub><sup>2−</sup>, NO<sub>3</sub><sup>−</sup> and NH<sub>4</sub><sup>+</sup> concentration

SO<sub>4</sub><sup>2−</sup> which is formed from the oxidation of SO<sub>2</sub>, is the predominant inorganic aerosol component. In general, SO<sub>4</sub><sup>2−</sup> concentrations show a strong positive response to the changes in SO<sub>2</sub> emissions (Butler and Lakens, 1991), though the SO<sub>2</sub> effective cloud oxidation rate can be affected by NH<sub>3</sub> (Pandis and Seinfeld, 1989; Tsimpidi et al., 2007). As a secondary species, SO<sub>4</sub><sup>2−</sup> is widely spread over the region, unlike SO<sub>2</sub> which is usually more localized to source areas. As seen in Table 2b, correlation coefficients for SO<sub>4</sub><sup>2−</sup> simulation (0.5–0.9) are higher than those for SO<sub>2</sub> (0.4–0.8). The NMBs for

25462

## Observations and modeling of air quality trends over 1990–2010 across the Northern Hemisphere

J. Xing et al.

Title Page

Abstract

Introduction

Conclusions

References

Tables

Figures

◀

▶

◀

▶

Back

Close

Full Screen / Esc

Printer-friendly Version

Interactive Discussion



## Observations and modeling of air quality trends over 1990–2010 across the Northern Hemisphere

J. Xing et al.

Title Page

Abstract

Introduction

Conclusions

References

Tables

Figures

◀

▶

◀

▶

Back

Close

Full Screen / Esc

Printer-friendly Version

Interactive Discussion



US-CASTNET (−8 to −45 %) and US-IMPROVE (−29 to 22 %) are comparable with the results reported by Zhang et al. (2009), which is −23 to 22 % and −8 to 16 %, Eder and Yu. (2006), which is −10 and −5 % on annual level, and Wang et al. (2009) ( $|NMB| < 55 %$ ). Significant  $SO_4^{2-}$  underestimation is noted during summer at both US-CASTNET (by 45.2 %) and US-IMPROVE (by 28.9 %). Such under-prediction in summer time has also been found in other modeling studies (Luo et al., 2011; Zhang et al., 2014). It might be associated with the uncertainty in precipitation and associated wet scavenging representation in the model. Better performance is shown at EU-EMEP, with NMB within  $\pm 30 %$ .

Worse performance for  $NO_3^-$  prediction is expected because of higher uncertainties in representing the gas/particle partitioning of airborne nitrate (Mathur and Dennis, 2003; Eder and Yu, 2006). Especially in summer when  $SO_4^{2-}$  concentrations are higher and available  $NH_3$  preferentially react to form ammonium sulfate, leading to low ambient  $NO_3^-$  level. Simulated and observed  $NO_3^-$  have the lowest correlations for both US-CASTNET and US-IMPROVE sites ( $R = 0.31$  and  $0.10$  respectively) during summer compared those in other seasons ( $R = 0.7$ ). Similar magnitudes of NMB (−56 to 59 %) and NME (89 to 197 %) at US-IMPROVE sites were reported by Wang et al. (2009) and Zhang et al. (2009). The underestimation in summer and overestimation in spring/winter are found relative to both CASTNET (NMB: −48 and 93/75 %) and IMPROVE (NMB: −41 and 107/95 %) and comparable to previous CMAQ analysis of Eder and Yu (2006) ( $|NMB| > 40 %$ ). Uncertainties in  $NH_3$  emission particularly in the seasonal temporal profile may also contribute to such bias characteristics. Slightly better performance is noted for  $NO_3^-$  at EU-EMEP sites, with higher  $R (> 0.6)$  and smaller bias (NMB: −67 to 23 %) for all seasons.

Performance for  $NH_4^+$  simulation is better than that of  $NO_3^-$  but slightly worse than for  $SO_4^{2-}$ . The NMB for US-CASTNET is −54 to 23 % which is comparable with Wang et al. (2009) ( $|NMB| < 50 %$ ). Similar performance statistics are shown for EU-EMEP (NMB: −15 to 68 %).

### 3.1.4 Elemental carbon (EC) concentration

EC being a primary pollutant, its spatial distributions exhibit strong correlation to its emissions. The correlation between the observed and simulated EC concentrations is high with  $R > 0.5$ , though the model significantly underestimates the concentrations because of the coarse resolution and also due to uncertainties of PM speciation profiles used to estimate the EC emissions. Such under-prediction has also been found in previous CMAQ modeling studies (Tesche et al., 2006; Appel et al., 2008). NMB up to -74 % which is worse than previous modeling studies utilizing relatively higher spatial resolution (Zhang et al., 2009; NMB = (-15.4 to 8 %); Eder and Yu, 2006; -6 %), but the magnitude of NMB is comparable with Wang et al. (2009) (NMB = 101.7 %) which also utilized coarse spatial resolution.

## 3.2 Trend analysis

Simulated trends in  $\text{SO}_2$ ,  $\text{NO}_2$ ,  $\text{O}_3$ ,  $\text{SO}_4^{2-}$ ,  $\text{NO}_3^-$ ,  $\text{NH}_4^+$  and EC concentrations in three regions (Eastern China, Eastern US and Europe) are given in Table 3. To help understand the changes, trends in input emissions used in this study are also provided in Table 3 as well as depicted in Fig. 2. Capability of the CMAQ model to capture the observed trends was examined through comparisons with network measurements, and both simulated and observed trends are quantified in Table 4 and Figs. 3–9.

### 3.2.1 $\text{SO}_2$ and $\text{NO}_2$ trend

Simulated trends in both  $\text{SO}_2$  and  $\text{NO}_2$  concentrations over the Northern Hemisphere reflect trends in  $\text{SO}_2$  and  $\text{NO}_x$  emissions, respectively (see Fig. 2a and b, Fig. 3a and Fig. 4a), with pronounced increasing trend in Asia and decreasing trend in Europe and North America. Particularly, in China annual change rates of  $\text{SO}_2$  and  $\text{NO}_2$  concentration are about 2.7 and 4.1 % which are comparable to their corresponding emission rates ( $\text{SO}_2$  and  $\text{NO}_x$ ) of 3.2 and 4.3 % respectively. Annual change rates of  $\text{SO}_2/\text{NO}_2$

concentrations in the US ( $-5.7/-1.4\%$ ) and Europe ( $-5.1/-1.2\%$ ) are also close to the rates of emission changes in both regions, at  $-5.4/-1.8$  and  $-5.4/-1.5\%$  respectively.

Such decreasing trends in the US and Europe are comparable with those inferred from observations at the different networks. The annual change rates of  $\text{SO}_2$  observed from US-CASTNET and US-AQS are  $-5.0$  and  $-5.5\%$ , close to that simulated by the model as  $-6.6$  and  $-6.0\%$ . Most of the reductions are located in the eastern US as seen in Fig. 3e and f. The model was unable to capture the increasing trend at two of the mid-east AQS sites and also the large decreasing trend at a few sites in the mid-west. It should be noted that the AQS  $\text{SO}_2$  measurements predominantly represent urban conditions, and the ability of a coarse resolution model in capturing  $\text{SO}_2$  levels and trends is influenced both by its inability to accurately represent sub-grid variability as well as changes in local emissions. For instance, the monitor in Kansas City, MO shows sharp increase in  $\text{SO}_2$  levels starting 2003; in contrast the grid averaged  $\text{SO}_2$  emissions in the corresponding model cell show systematic decreasing trends over the 21 year period resulting in the simulated decreasing  $\text{SO}_2$  trend at this location. Also, as seen in the scatter plots in these panels, the pathway of such reductions from 1990 to 2010 is in good agreement between observation and simulation. Stronger trends are noted in winter when  $\text{SO}_2$  concentrations are higher compared to other seasons in both observed ( $-0.368 \mu\text{g m}^{-3} \text{yr}^{-1}$ ) and simulated trend ( $-0.366 \mu\text{g m}^{-3} \text{yr}^{-1}$ ) at US-CASTNET (see Table 4). Annual change rates of  $\text{SO}_2$  observed from EU-AIRBASE and EU-EMEP are  $-8.7$  and  $-7.3\%$  which are close to that simulated by the model at  $-6.6$  and  $-6.1\%$ , with higher rates in winter when  $\text{SO}_2$  concentration are at their highest level. Significant reductions are found at locations in Southern UK, Benelux, Germany, Italy, Czech Republic, Poland, Hungary and Romania.

The overall reductions in  $\text{NO}_2$  from 1990 to 2010 are also in good agreement between the observations and model simulations. Observed decreasing trends of  $\text{NO}_2$  concentrations (and annual change rate) are shown in urban networks, i.e., US-AQS and EU-AIRBASE are  $-0.91 \mu\text{g m}^{-3} \text{yr}^{-1}$  ( $-2.8\%$ ) and  $-0.59 \mu\text{g m}^{-3} \text{yr}^{-1}$  ( $-1.8\%$ ) respectively. Model simulated trends (and annual change rate) at these two urban

## Observations and modeling of air quality trends over 1990–2010 across the Northern Hemisphere

J. Xing et al.

Title Page

Abstract

Introduction

Conclusions

References

Tables

Figures

◀

▶

◀

▶

Back

Close

Full Screen / Esc

Printer-friendly Version

Interactive Discussion



**Observations and modeling of air quality trends over 1990–2010 across the Northern Hemisphere**

J. Xing et al.

Title Page

Abstract

Introduction

Conclusions

References

Tables

Figures

◀

▶

◀

▶

Back

Close

Full Screen / Esc

Printer-friendly Version

Interactive Discussion

$O_3$  chemistry is likely to be at  $NO_x$ -limited regime during periods of heavy photochemical pollution (Trainer et al., 1993; Xing et al., 2011b), suggesting that  $NO_x$  controls are more effective in reducing annual maximum (rather than average) of DM8  $O_3$ . Therefore, trends in  $NO_x$  emission are more likely to have positive correlation with trends in annual maximum (rather than average) of DM8  $O_3$ . As expected, simulated trend of annual maximum of DM8  $O_3$  concentration (see Fig. 5a) looks quite similar to the  $NO_x$  and VOC emission trends (Fig. 2b and c). The simulated annual increasing rate of annual maximum of DM8  $O_3$  in eastern China is 1.49%, which is associated with the increase in  $NO_x$  and VOC emissions (by 4.3 and 2.3% per year). In contrast, due to reductions of emissions, substantial decreasing trends in annual maximum of DM8  $O_3$  are apparent in both the eastern US and Europe, with magnitudes of  $-0.66$  and  $-0.54$ % per year, respectively (see Table 3). Significant increases of  $O_3$  are also shown in northern India, west-Asia and sub-Saharan Africa where both  $NO_x$  and VOC emissions have increased during this period (see Fig. 2b and c).

Observed decreasing trends in annual maximum of DM8  $O_3$  concentrations (and annual change rate) in EU-EMEP, EU-AIRBASE and US-CASTNET are  $-1.07 \mu\text{g m}^{-3} \text{yr}^{-1}$  ( $-0.7\%$ ),  $-1.35 \mu\text{g m}^{-3} \text{yr}^{-1}$  ( $-0.8\%$ ) and  $-1.86 \mu\text{g m}^{-3} \text{yr}^{-1}$  ( $-1.1\%$ ) respectively. Similar trends are estimated by the model simulation for both networks, i.e.,  $-1.31 \mu\text{g m}^{-3} \text{yr}^{-1}$  ( $-0.9\%$ ),  $-2.13 \mu\text{g m}^{-3} \text{yr}^{-1}$  ( $-1.1\%$ ) and  $-0.95 \mu\text{g m}^{-3} \text{yr}^{-1}$  ( $-0.6\%$ ) (see Table 4). The failure to capture the slightly increasing trends in observations at urban network (i.e., EU-AIRBASE) might be associated with the limitation by coarse spatial resolution that causes the model fail to represent the VOC-limited regime at these urban locations and a likely switch of  $O_3$  chemistry from  $NO_x$ - to VOC-limited regime which usually goes along with the transition from urban to rural area (e.g., Xing et al., 2011b). Such decreasing trends are noted in all seasons except during winter when  $O_3$  is at the lowest level. In contrast, the most significant reduction occurred in summer when  $O_3$  concentrations are at the highest. The spatial pattern of  $O_3$  trends is quite similar to that of  $NO_2$ , with more pronounced decrease in regions downwind of urban areas across the eastern US and California as

## Observations and modeling of air quality trends over 1990–2010 across the Northern Hemisphere

J. Xing et al.

Title Page

Abstract

Introduction

Conclusions

References

Tables

Figures

◀

▶

◀

▶

Back

Close

Full Screen / Esc

Printer-friendly Version

Interactive Discussion

well as Southern UK, Northern France, Benelux and Germany. The reason for increasing trends shown in both observed and model in mid-west of US might be explained by the changes in local emissions (less or no controls in mid-west) as well as increasing long-range transport of pollutants across the Pacific (Mathur et al., 2014). Analysis of long-term observations at remote sites along the western US (e.g., Jaffe and Ray, 2007; Parrish et al., 2009) also show increasing trends in O<sub>3</sub> within the boundary layer attributable to inflow to the western US from the Pacific.

Though long-term observation records of O<sub>3</sub> are not available in China, recent studies have suggested increasing trends similar to those found here. For instance, Xu et al. (2011) suggested significant increasing trends in tropospheric ozone residual over the North China Plain. Ding et al. (2008) suggest that O<sub>3</sub> in the lower troposphere over Beijing had a strong positive trend (2 % per year) during the period 1995 to 2005. Ozone-sonde measurements analyzed by Wang et al. (2012) suggests a clear positive trend in the maximum summer ozone concentration (3.4 % per year) over the Beijing area during 2002–2010. In this study, the trend in summer maximum of DM8 ozone concentration in Beijing during 1990 to 2010 is estimated to be 2 % per year, which is comparable to that inferred from observations in these two recent studies.

Observation records at three sites in WDCGG network were used to investigate trends in O<sub>3</sub> distribution in eastern Asia. One of these sites, Minamitorishima (noted as S1, lat: 24.28° N, lon: 153.98° E), is located far from land and can be considered to be a representative of clean conditions, while two sites located on Honshu island, i.e., Tsukuba (noted as S2, lat: 36.05, lon: 140.13) which is to the northwest of Tokyo and closest to urban regions, and Ryori (noted as S3, lat: 39.03, lon: 141.82) which is in the north and representative of rural conditions. The model generally captured the observed pattern of O<sub>3</sub> trends at each site. For the clean site (S1), no significant trends are inferred either in the observed or the simulated maximum of DM8 O<sub>3</sub>. However, for the urban site (S2), significant reduction, particularly during summer, is noted in the observed values and is reflective of emission reductions in Japan during past two decades (e.g., Wakamatsu et al., 2013). In contrast, increasing trends are inferred at



## Observations and modeling of air quality trends over 1990–2010 across the Northern Hemisphere

J. Xing et al.

Title Page

Abstract

Introduction

Conclusions

References

Tables

Figures

◀

▶

◀

▶

Back

Close

Full Screen / Esc

Printer-friendly Version

Interactive Discussion

in both  $\text{NO}_x$  and  $\text{NH}_3$  emissions results in the increasing trend in airborne  $\text{NO}_3^-$  in China (5.4 % per year), while reductions in emissions of both results in the decreasing trend in Europe (−1.8 % per year). In contrast, over the past two decades in the US, a reduction in  $\text{SO}_2$  and  $\text{NO}_x$  accompanied with a growth in  $\text{NH}_3$  emission results in different trends across different seasons. The model fails to reproduce the decreasing trend in  $\text{NO}_3^-$  at both US-CASTNET and US-IMPROVE in spring, summer and fall though the significance of the trend is small. However, both simulated and observed  $\text{NO}_3^-$  show an increasing trend in winter values when  $\text{NO}_3^-$  is at the highest level. Similar observed increasing trend is noted during winter at the EU-EMEP monitors, which is not captured by the model. The decreasing trend at the EU-EMEP locations during other seasons is however captured by the model. Successful reproduction of  $\text{NO}_3^-$  trends depends on an accurate baseline emission as well as an accurate representation of changes in historical  $\text{NH}_3$  emission. Unfortunately, both current  $\text{NH}_3$  emission and their historical trends over the globe still suffer from large uncertainties (e.g., Heald et al., 2012) and likely contribute to the significant bias in the simulated  $\text{NO}_3^-$  trend.

$\text{NH}_4^+$  is simulated based on the thermodynamic equilibrium between the  $\text{NO}_x$ – $\text{SO}_x$ – $\text{NH}_x$  species. It shows a similar increasing trend in China (3.4 %) and a decreasing trend in the US (−0.7 %) and Europe (−2.9 %), as illustrated in Fig. 8.  $\text{NH}_4^+$  simulation suffers the same uncertainties as  $\text{NO}_3^-$  which leads to difficulties in reproducing the trend in observations (see Table 4).

### 3.2.4 Elemental carbon (EC) trends

Growth of human activities such as biomass burning and open fires results in the simulated increasing trends in EC levels in China (1.0%; see Table 3), India and sub-Saharan Africa (see Fig. 9). In contrast, continuous controls have led to a decreasing trend in EC concentrations in the US (−3.4 %) and Europe (−2.5 %). The observed trend in EC at US-IMPROVE, i.e.,  $-0.006 \mu\text{g m}^{-3} \text{yr}^{-1}$  (−2.6 %) is well reproduced by the model, i.e.,  $-0.003 \mu\text{g m}^{-3} \text{yr}^{-1}$  (−3.3 %). Both observations and the model suggest

higher magnitudes of trends during fall and winter, and are likely associated with higher ambient levels during these seasons.

Decreasing trend of EC in Europe has also been observed in other studies (Järvi et al., 2008). The model estimates a consistent decreasing EC trend in the Canadian Arctic (see Fig. 9) which is mainly impacted by emissions from Europe and Russia during winter and spring as demonstrated by Sharma et al. (2004) who analyzed in-situ ground-level observations of aerosol black carbon between 1989 and 2002. The increasing trend of EC in southern Asia is corroborated by the evidence found from the Nam Co Lake (located in the central Tibetan Plateau) sediments indicating a recent rise in BC deposition flux (Cong et al., 2013).

## 4 Discussion

### 4.1 O<sub>3</sub> chemistry

As discussed in Sect. 3.2.2, the response of O<sub>3</sub> concentration depends on changes in NO<sub>x</sub> and VOC emissions, and the non-linear chemistry associated with the subsequent VOC- or NO<sub>x</sub>-limited environment. The response of O<sub>3</sub> to changing levels of NO<sub>x</sub> and VOC have previously been examined through a variety of methods ranging from isopleths created from chemistry box-model calculations to detailed spatially varying response surfaces developed from output of hundreds of simulations with detailed air pollution modeling systems (e.g., Xing et al., 2011b). Exploration of the changes in O<sub>3</sub> levels in response to historical (and geographically varying) changes in NO<sub>x</sub> and VOC emissions, as captured by the multi-decadal simulations presented here, provide a unique opportunity to develop insights into factors controlling changes in O<sub>3</sub> production and distributions.

Figure 10 attempts to summarize the changes in NO<sub>x</sub> and VOC emissions as well as the surface O<sub>3</sub> response during the 1990–2010 period for the three regions; the figures in the left panel illustrate the changes in emissions relative to the 1990 values



reductions in the region on reducing peak O<sub>3</sub> during regional pollution episodes. During the period 2000–2007 when solely VOC emissions reduced (–10%), no significant reduction in either annual maximum or average of DM8 O<sub>3</sub> occurred. Reductions in NO<sub>x</sub> (–10%) with VOC (–5%) emissions in the subsequent 2007 to 2010 period lead to reductions in both maximum and average of DM8 O<sub>3</sub>.

## 4.2 PM chemistry

The nonlinear response of NO<sub>3</sub><sup>–</sup> concentration to SO<sub>2</sub>, NO<sub>x</sub> and NH<sub>3</sub> emissions are well documented (e.g., Mathur and Dennis, 2003; Tsimpidi et al., 2007; Makar et al., 2009). Figure 11 attempts to summarize the changes in emissions and factors driving the NO<sub>x</sub>–SO<sub>x</sub>–NH<sub>x</sub> system and its influence on changing inorganic particulate matter composition for the three regions. Contrasting trends in emissions over the past two decades in the three regions are apparent: while China and many growing regions of Asia have witnessed significant increases in emissions of NO<sub>x</sub>, SO<sub>2</sub>, and NH<sub>3</sub>, significant reductions in emissions of all these species have occurred in Europe. In contrast in the eastern US, while combustion related emissions of NO<sub>x</sub> and SO<sub>2</sub> have declined, growth in agricultural animal husbandry have resulted in significant increases in NH<sub>3</sub> emissions. To examine the impact of the varying emissions patterns on inorganic particulate matter formation and composition in these regions, we examined trends in two metrics relative to their 1990 values: (i) the degree of sulfate neutralization, an estimate of the neutralization of sulfate by ammonium (Pinder et al., 2008b;  $DSN = ([NH_4^+] - [NO_3^-]) / [SO_4^{2-}]$ ), and (ii) a new metric, the “nitration ratio (NR)” (i.e., NO<sub>3</sub><sup>–</sup> concentration divided by NO<sub>x</sub> emission) to represent the relative amount of oxidized-N emissions that is eventually transformed to aerosol NO<sub>3</sub><sup>–</sup>, changes in the ratio could thus be viewed as an indicator of the relative effectiveness of NO<sub>x</sub> controls for given conditions. Figure 11 presents the response of PM chemistry to the changes in emissions as indicated by the trends in these metric during the period 1990–2010.



## 5 Conclusion

Trends in air quality across the Northern Hemisphere from 1990 to 2010 have been simulated by the WRF-CMAQ model driven with a representation of historical emission inventories derived from the EDGAR. Thorough comparison with several surface observation networks mostly in Europe and North American has been conducted. Significant contrasting changes in emissions have occurred across the Northern Hemisphere over the past two decades with reductions in North America and Western Europe resulting from control measures on combustion related sources and increases across large parts of Asia associated with economic and population growth. Model calculations show associated contrasting trends in air pollution across the Northern Hemisphere emphasizing the changing tropospheric composition of trace pollutants as well as the potentially changing background pollution levels in different regions resulting from changes in the amounts of long-range transported pollution. The model is generally able to capture the observed trends in air pollution and performance statistics are comparable with results from other studies in regions across the Northern Hemisphere. However, the model estimates still suffer from uncertainties in emissions (in regards to temporal variation and speciation), coarse spatial resolution and subsequent impacts on representation of non-linear atmospheric chemistry. The lack of long-term observations in Asia, particularly over China and India limits a robust model performance evaluation in these polluted areas.

Model simulated air quality trends over the past two decades largely agree with those derived from observations. Significant reduction in ambient levels of most pollutants is seen in the US and Europe resulting from emission controls implemented during 1990–2010, while levels of all pollutants in China show pronounced increasing trends during the same period. Examining the simulated and observed historical trends in atmospheric chemistry can help guide development of future air pollution abatement strategies. Model calculations over the 1990–2010 period suggest that in the relative amounts of VOC and NO<sub>x</sub> emission controls in different regions across the

## Observations and modeling of air quality trends over 1990–2010 across the Northern Hemisphere

J. Xing et al.

Title Page

Abstract

Introduction

Conclusions

References

Tables

Figures



Back

Close

Full Screen / Esc

Printer-friendly Version

Interactive Discussion



## Observations and modeling of air quality trends over 1990–2010 across the Northern Hemisphere

J. Xing et al.

Title Page

Abstract

Introduction

Conclusions

References

Tables

Figures

◀

▶

◀

▶

Back

Close

Full Screen / Esc

Printer-friendly Version

Interactive Discussion

Northern Hemisphere (east US, Europe, and China), have led to significantly different trends in tropospheric O<sub>3</sub> in these regions. In particular, steady increase in NO<sub>x</sub> and VOC emissions (with a ratio of 0.46 relative to 1990 emissions) in China have resulted in a near-linear increase in surface O<sub>3</sub> concentrations in the region, suggesting that possible control strategies that maintain this relative ration could potentially be most effective in avoiding non-linear response resulting from VOC-limitation of alternate approaches. Differences in the historical changes in the relative amounts of NH<sub>3</sub>, NO<sub>x</sub>, and SO<sub>2</sub> emissions in these regions also impact the trends in inorganic particulate matter amounts and composition in these regions. In particular, the amount of particulate nitrate formed per unit of NO<sub>x</sub> emissions is influenced by changing NH<sub>3</sub> emissions and could be important in assessing the relative effectiveness of different control strategies. Simultaneous growth of NH<sub>3</sub> emission along with those of NO<sub>x</sub> and SO<sub>2</sub> in China over the past 2 decades has resulted in the increasing particulate nitrate formation trends in the region. In contrast, in the eastern US the relative fraction of NO<sub>x</sub> converted to particulate nitrate exhibits a steady increase over the past two decades suggesting an offset in the relative effectiveness of control measures on particulate nitrate levels in the region. Simultaneous reductions in NH<sub>3</sub> emissions along with those of NO<sub>x</sub>, and SO<sub>2</sub> in west Europe over the past two decades resulted in no significant trend in nitration ratio, suggesting effectiveness of the overall measures in terms of particulate nitrate levels in the region.

*Acknowledgements.* Although this work has been reviewed and approved for publication by the US Environmental Protection Agency (EPA), it does not reflect the views and policies of the agency. This work was supported in part by an inter-agency agreement between the US Department of Energy project (IA number is DE-SC000378) and the US EPA (IA number is RW-89-9233260 1). This research was performed while Jia Xing held a National Research Council Research Associateship Award at US EPA. The authors gratefully acknowledge the free availability and use of datasets associated with the EDGAR, SMOKE, GEIA, CASTNET, IMPROVE, AQS, EMEP, AIRBASE, WDCGG and China API initiatives.

## References

- Akimoto, H., Ohara, T., Kurokawa, J. I., and Horii, N.: Verification of energy consumption in China during 1996–2003 by using satellite observational data, *Atmos. Environ.*, 40, 7663–7667, 2006.
- 5 Appel, K. W., Gilliland, A. B., Sarwar, G., and Gilliam, R. C.: Evaluation of the Community Multiscale Air Quality (CMAQ) model version 4.5: sensitivities impacting model performance: Part I – Ozone, *Atmos. Environ.*, 41, 9603–9615, 2007.
- Appel, K. W., Bhave, P. V., Gilliland, A. B., Sarwar, G., and Roselle, S. J.: Evaluation of the community multiscale air quality (CMAQ) model version 4.5: sensitivities impacting model performance; Part II – Particulate matter, *Atmos. Environ.*, 42, 6057–6066, 2008.
- 10 Binkowski, F. S. and Roselle, S. J.: Community Multiscale Air Quality (CMAQ) model aerosol component, I: Model description, *J. Geophys. Res.*, 108, 4183, doi:10.1029/2001JD001409, 2003.
- Blanchard, C. L., Tanenbaum, S., and Hidy, G. M.: Effects of sulfur dioxide and oxides of nitrogen emission reductions on fine particulate matter mass concentrations: regional comparisons, *JAPCA J. Air Waste Ma.*, 57, 1337–1350, 2007.
- Butler, T. J. and Lakens, G. E.: The impact of changing regional emissions on precipitation chemistry in the eastern United States, *Atmos. Environ. A-Gen.*, 25, 305–315, 1991.
- Byun, D. and Schere, K. L.: Review of the governing equations, computational algorithms, and other components of the Models-3 Community Multiscale Air Quality (CMAQ) modeling system, *Appl. Mech. Rev.*, 59, 51–77, 2006.
- 20 Chameides, W. L., Fehsenfeld, F., Rodgers, M. O., Cardelino, C., Martinez, J., Parrish, D., Loneman, W., Lawson, D. R., Rasmussen, R. A., Zimmerman, P., Greenberg, J., Middleton, P., and Wang, T.: Ozone precursor relationships in the ambient atmosphere, *J. Geophys. Res.-Atmos.*, 97, 6037–6055, 1992.
- 25 Civerolo, K., Hogrefe, C., Zalewsky, E., Hao, W., Sistla, G., Lynn, B., Rosenzweig, C., and Kinney, P. L.: Evaluation of an 18-year CMAQ simulation: seasonal variations and long-term temporal changes in sulfate and nitrate, *Atmos. Environ.*, 44, 4745–3752, 2010.
- Colette, A., Granier, C., Hodnebrog, Ø., Jakobs, H., Maurizi, A., Nyiri, A., Bessagnet, B., D'Angiola, A., D'Isidoro, M., Gauss, M., Meleux, F., Memmesheimer, M., Mieville, A., Rouil, L., Russo, F., Solberg, S., Stordal, F., and Tampieri, F.: Air quality trends in Europe over
- 30

**Observations and modeling of air quality trends over 1990–2010 across the Northern Hemisphere**

J. Xing et al.

Title Page

Abstract

Introduction

Conclusions

References

Tables

Figures



Back

Close

Full Screen / Esc

Printer-friendly Version

Interactive Discussion



## Observations and modeling of air quality trends over 1990–2010 across the Northern Hemisphere

J. Xing et al.

Title Page

Abstract

Introduction

Conclusions

References

Tables

Figures

◀

▶

◀

▶

Back

Close

Full Screen / Esc

Printer-friendly Version

Interactive Discussion



the past decade: a first multi-model assessment, *Atmos. Chem. Phys.*, 11, 11657–11678, doi:10.5194/acp-11-11657-2011, 2011.

Cong, Z., Kang, S., Gao, S., Zhang, Y., Li, Q., and Kawamura, K.: Historical trends of atmospheric black carbon on Tibetan Plateau as reconstructed from a 150-year lake sediment record, *Environ. Sci. Technol.*, 47, 2579–2586, 2013.

Ding, A. J., Wang, T., Thouret, V., Cammas, J.-P., and Nédélec, P.: Tropospheric ozone climatology over Beijing: analysis of aircraft data from the MOZAIC program, *Atmos. Chem. Phys.*, 8, 1–13, doi:10.5194/acp-8-1-2008, 2008.

Eder, B. and Yu, S.: A performance evaluation of the 2004 release of Models-3 CMAQ, *Atmos. Environ.*, 40, 4811–4824, 2006.

EEA (European Environment Agency): European Union Emission Inventory Report 1990–2010 under the UNECE Convention on Long-range Transboundary Air Pollution (LRTAP), EEA Technical report, 30 July, Copenhagen, Denmark, doi:10.2800/5219, 2012.

European Commission: Joint Research Centre (JRC)/Netherlands Environmental Assessment Agency (PBL). Emission Database for Global Atmospheric Research (EDGAR), release version 4.2., available at: <http://edgar.jrc.ec.europa.eu> (last access: 25 September 2014), 2011.

Foley, K. M., Roselle, S. J., Appel, K. W., Bhawe, P. V., Pleim, J. E., Otte, T. L., Mathur, R., Sarwar, G., Young, J. O., Gilliam, R. C., Nolte, C. G., Kelly, J. T., Gilliland, A. B., and Bash, J. O.: Incremental testing of the Community Multiscale Air Quality (CMAQ) modeling system version 4.7, *Geosci. Model Dev.*, 3, 205–226, doi:10.5194/gmd-3-205-2010, 2010.

Gan, C.-M., Pleim, J., Mathur, R., Hogrefe, C., Long, C. N., Xing, J., Roselle, S., and Wei, C.: Assessment of the effect of air pollution controls on trends in shortwave radiation over the United States from 1995 through 2010 from multiple observation networks, *Atmos. Chem. Phys.*, 14, 1701–1715, doi:10.5194/acp-14-1701-2014, 2014.

Guenther, A., Hewitt, C. N., Erickson, D., Fall, R., Geron, C., Graedel, T., Harley, P., Klinger, L., Lerdau, M., McKay, W. A., Pierce, T., Scholes, B., Steinbrecher, R., Tallamraju, R., Taylor, J., and Zimmerman, P.: A global model of natural volatile organic compound emissions, *J. Geophys. Res.*, 100, 8873–8892, 1995.

He, K. B.: Multi-resolution Emission Inventory for China (MEIC): Model Framework and 1990–2010 Anthropogenic Emissions, International Global Atmospheric Chemistry Conference, Beijing, China, 17–21 September, S1-I-2, 2012.

Heald, C. L., Collett Jr., J. L., Lee, T., Benedict, K. B., Schwandner, F. M., Li, Y., Clarisse, L., Hurtmans, D. R., Van Damme, M., Clerbaux, C., Coheur, P.-F., Philip, S., Martin, R. V., and

**Observations and modeling of air quality trends over 1990–2010 across the Northern Hemisphere**

J. Xing et al.

[Title Page](#)[Abstract](#)[Introduction](#)[Conclusions](#)[References](#)[Tables](#)[Figures](#)[◀](#)[▶](#)[◀](#)[▶](#)[Back](#)[Close](#)[Full Screen / Esc](#)[Printer-friendly Version](#)[Interactive Discussion](#)

Pye, H. O. T.: Atmospheric ammonia and particulate inorganic nitrogen over the United States, *Atmos. Chem. Phys.*, 12, 10295–10312, doi:10.5194/acp-12-10295-2012, 2012.

Hogrefe, C., Lynn, B., Goldberg, R., Rosenzweig, C., Zalewsky, E., Hao, W., Doraiswamy, P., Civerolo, K., Ku, J.-Y., Sistla, G., and Kinney, P. L.: A combined model-observation approach to estimate historic gridded fields of PM<sub>2.5</sub> mass and species concentrations, *Atmos. Environ.*, 43, 2561–2570, 2009.

Hogrefe, C., Hao, W., Zalewsky, E. E., Ku, J.-Y., Lynn, B., Rosenzweig, C., Schultz, M. G., Rast, S., Newchurch, M. J., Wang, L., Kinney, P. L., and Sistla, G.: An analysis of long-term regional-scale ozone simulations over the Northeastern United States: variability and trends, *Atmos. Chem. Phys.*, 11, 567–582, doi:10.5194/acp-11-567-2011, 2011.

Iacono, M. J., Delamere, J. S., Mlawer, E. J., Shephard, M. W., Clough, S. A., and Collins, W. D.: Radiative forcing by long-lived greenhouse gases: calculations with the AER radiative transfer models, *J. Geophys. Res.*, 113, D13103, doi:10.1029/2008JD009944, 2008.

Irie, H., Sudo, K., Akimoto, H., Richter, A., Burrows, J. P., Wagner, T., Wenig, M., Beirle, S., Kondo, Y., Sinyakov, V. P., and Goutail, F.: Evaluation of long-term tropospheric NO<sub>2</sub> data obtained by GOME over East Asia in 1996–2002, *Geophys. Res. Lett.*, 32, L11810, doi:10.1029/2005GL022770, 2005.

Jaffe, D. and Ray, J.: Increase in surface ozone at rural sites in the western US, *Atmos. Environ.*, 41, 5452–5463, 2007.

Janssens-Maenhout, G., Dentener, F., Van Aardenne, J., Monni, S., Pagliari, V., Orlandini, L., Klimont, Z., Kurokawa, J., Akimoto, H., Ohara, T., Wankmueller, R., Battye, B., Grano, D., Zuber, A., and Keating, T.: EDGAR-HTAP: a Harmonized Gridded Air Pollution Emission Dataset Based on National Inventories, EUR report No EUR 25229, European Commission Publications Office, Ispra, Italy, 2012.

Järvi, L., Junninen, H., Karppinen, A., Hillamo, R., Virkkula, A., Mäkelä, T., Pakkanen, T., and Kulmala, M.: Temporal variations in black carbon concentrations with different time scales in Helsinki during 1996–2005, *Atmos. Chem. Phys.*, 8, 1017–1027, doi:10.5194/acp-8-1017-2008, 2008.

Jiang, D. H., Zhang, Y., Hu, X., Zeng, Y., Tan, J. G., Shao, D. M.: Progress in developing an ANN model for air pollution index forecasting, *Atmos. Environ.*, 28, 7055–7064, 2004.

Koumoutsaris, S. and Bey, I.: Can a global model reproduce observed trends in summertime surface ozone levels?, *Atmos. Chem. Phys.*, 12, 6983–6998, doi:10.5194/acp-12-6983-2012, 2012.

**Observations and modeling of air quality trends over 1990–2010 across the Northern Hemisphere**

J. Xing et al.

Title Page

Abstract

Introduction

Conclusions

References

Tables

Figures

◀

▶

◀

▶

Back

Close

Full Screen / Esc

Printer-friendly Version

Interactive Discussion



- Kukkonen, J., Olsson, T., Schultz, D. M., Baklanov, A., Klein, T., Miranda, A. I., Monteiro, A., Hirtl, M., Tarvainen, V., Boy, M., Peuch, V.-H., Poupkou, A., Kioutsioukis, I., Finardi, S., Sofiev, M., Sokhi, R., Lehtinen, K. E. J., Karatzas, K., San José, R., Astitha, M., Kallos, G., Schaap, M., Reimer, E., Jakobs, H., and Eben, K.: A review of operational, regional-scale, chemical weather forecasting models in Europe, *Atmos. Chem. Phys.*, 12, 1–87, doi:10.5194/acp-12-1-2012, 2012.
- Logan, J. A., Staehelin, J., Megretskaia, I. A., Cammas, J.-P., Thouret, V., Claude, H., De Backer, H., Steinbacher, M., Scheel, H. E., Stübi, R., Fröhlich, M., and Derwent, R.: Changes in ozone over Europe: analysis of ozone measurements from sondes, regular aircraft (MOZAIC) and alpine surface sites, *J. Geophys. Res.*, 117, D09301, doi:10.1029/2011JD016952, 2012.
- Luo, C., Wang, Y. H., Mueller, S., and Knipping, E.: Diagnosis of an underestimation of summertime sulfate using the Community Multiscale Air Quality model, *Atmos. Environ.*, 45, 5119–5130, 2011.
- Makar, P. A., Moran, M. D., Zheng, Q., Cousineau, S., Sassi, M., Duhamel, A., Besner, M., Davignon, D., Crevier, L.-P., and Bouchet, V. S.: Modelling the impacts of ammonia emissions reductions on North American air quality, *Atmos. Chem. Phys.*, 9, 7183–7212, doi:10.5194/acp-9-7183-2009, 2009.
- Mathur, R. and Dennis, R. L.: Seasonal and annual modeling of reduced nitrogen compounds over the eastern United States: emissions, ambient levels, and deposition amounts, *J. Geophys. Res.-Atmos.*, 108, 4481, doi:10.1029/2002JD002794, 2003.
- Mathur, R., Yu, S., Kang, D., and Schere, K. L.: Assessment of the wintertime performance of developmental particulate matter forecasts with the Eta-Multiscale Air Quality modeling system, *J. Geophys. Res.-Atmos.*, 113, D02303, doi:10.1029/2007JD008580, 2008.
- Mathur, R., Gilliam, R., Bullock, O. R., Roselle, S., Pleim, J., Wong, D., Binkowski, F., and Streets, D.: Extending the applicability of the community multiscale air quality model to hemispheric scales: motivation, challenges, and progress, in: *Air Pollution Modeling and its Applications*, vol. XXI, edited by: Steyn, D. G. and Trini, S., Springer, Dordrecht, 175–179, 2012.
- Mathur, R., Roselle, S., Young, J., and Kang, D.: Representing the effects of long-range transport and lateral boundary conditions in regional air pollution models, *Air Pollution Modeling and its Application XXII*, NATO Sci. Peace Secur., Springer, Heidelberg, Germany, Chapter 51, 303–308, 2014.

**Observations and modeling of air quality trends over 1990–2010 across the Northern Hemisphere**

J. Xing et al.

Title Page

Abstract

Introduction

Conclusions

References

Tables

Figures

◀

▶

◀

▶

Back

Close

Full Screen / Esc

Printer-friendly Version

Interactive Discussion



Matthias, V., Aulinger, A., Bieser, J., Cuesta, J., Geyer, B., Langmann, B., Serikov, I., Mattis, I., Minikin, A., Mona, L., Quante, M., Schumann, U., and Weinzierl, B.: The ash dispersion over Europe during the Eyjafjallajökull eruption – comparison of CMAQ simulations to remote sensing and air-borne in-situ observations, *Atmos. Environ.*, 48, 184–194, 2012.

Ott, L. E., Pickering, K. E., Stenichikov, G. L., Allen, D. J., De-Caria, A. J., Ridley, B., Lin, R.-F., Lang, S., and Tao, W.-K.: Production of lightning NO<sub>x</sub> and its vertical distribution calculated from three-dimensional cloud-scale chemical transport model simulations, *J. Geophys. Res.-Atmos.*, 115, D04301, doi:10.1029/2009jd011880, 2010.

Pandis, S. N. and Seinfeld, J. H.: Sensitivity analysis of a chemical mechanism for aqueous-phase atmospheric chemistry, *J. Geophys. Res.-Atmos.*, 94, 1105–1126, 1989.

Parrish, D. D., Millet, D. B., and Goldstein, A. H.: Increasing ozone in marine boundary layer inflow at the west coasts of North America and Europe, *Atmos. Chem. Phys.*, 9, 1303–1323, doi:10.5194/acp-9-1303-2009, 2009.

Parrish, D. D., Law, K. S., Staehelin, J., Derwent, R., Cooper, O. R., Tanimoto, H., Volz-Thomas, A., Gilge, S., Scheel, H.-E., Steinbacher, M., and Chan, E.: Long-term changes in lower tropospheric baseline ozone concentrations at northern mid-latitudes, *Atmos. Chem. Phys.*, 12, 11485–11504, doi:10.5194/acp-12-11485-2012, 2012.

Parrish, D. D., Lamarque, J. F., Naik, V., Horowitz, L., Shindell, D. T., Staehelin, J., Derwent, R., Cooper, O. R., Tanimoto, H., Volz-Thomas, A., Gilge, S., Scheel, H.-E., Steinbacher, M., and Fröhlich, M.: Long-term changes in lower tropospheric baseline ozone concentrations: comparing chemistry–climate models and observations at northern midlatitudes, *J. Geophys. Res.-Atmos.*, 119, 5719–5736, 2014.

Pinder, R. W., Gilliland, A. B., and Dennis, R. L.: Environmental impact of atmospheric NH<sub>3</sub> emissions under present and future conditions in the eastern United States, *Geophys. Res. Lett.*, 35, L12808, doi:10.1029/2008GL033732, 2008a.

Pinder, R. W., Dennis, R. L., and Bhave, P. V.: Observable indicators of the sensitivity of PM<sub>2.5</sub> nitrate to emission reductions – Part I: Derivation of the adjusted gas ratio and applicability at regulatory-relevant time scales, *Atmos. Environ.*, 42, 1275–1286, 2008b.

Pleim, J. E.: A combined local and nonlocal closure model for the atmospheric boundary layer. Part I: Model description and testing, *J. Appl. Meteorol. Clim.*, 46, 1383–1395, doi:10.1175/JAM2539.1, 2007a.

## Observations and modeling of air quality trends over 1990–2010 across the Northern Hemisphere

J. Xing et al.

Title Page

Abstract

Introduction

Conclusions

References

Tables

Figures

◀

▶

◀

▶

Back

Close

Full Screen / Esc

Printer-friendly Version

Interactive Discussion



Pleim, J. E.: A combined local and nonlocal closure model for the atmospheric boundary layer. Part II: Application and evaluation in a mesoscale meteorological model, *J. Appl. Meteorol. Clim.*, 46, 1396–1409, doi:10.1175/JAM2534.1, 2007b.

Pleim, J. E. and Gilliam, R.: An indirect data assimilation scheme for deep soil temperature in the Pleim–Xiu land surface model, *J. Appl. Meteorol. Clim.*, 48, 1362–1376, 2009.

Pleim, J. E. and Xiu, A.: Development and testing of a surface flux and planetary boundary layer model for application in mesoscale models, *J. Appl. Meteorol.*, 34, 16–32, 1995.

Pleim, J. E. and Xiu, A.: Development of a land surface model. Part II: Data Assimilation, *J. Appl. Meteorol.*, 42, 1811–1822, 2003.

Price, C., Penner, J., and Prather, M.: NO<sub>x</sub> from lightning 1: global distribution based on lightning physics, *J. Geophys. Res.*, 102, 5929–5941, 1997.

Richter, A., Burrows, J. P., Nues, H., Granier, C., and Niemeier, U.: Increase in tropospheric nitrogen dioxide over China observed from space, *Nature*, 437, 129–132, 2005.

Sharma, S., Lavoué, D., Cachier, H., Barrie, L. A., and Gong, S. L.: Long-term trends of the black carbon concentrations in the Canadian Arctic, *J. Geophys. Res.-Atmos.*, 109, D15203, doi:10.1029/2003JD004331, 2004.

Sickles II, J. E. and Shadwick, D. S.: Changes in air quality and atmospheric deposition in the eastern United States: 1990–2004, *J. Geophys. Res.*, 112, D17302, doi:10.1029/2006JD007843, 2007.

Sillman, S.: The relation between ozone, NO<sub>x</sub> and hydrocarbons in urban and polluted rural environments, *Atmos. Environ.*, 33, 1821–1845, 1999.

Simpson, D., Fagerli, H., Jonson, J. E., Tsyro, S., Wind, P., and Tuovinen, J.: Transboundary Acidification, Eutrophication, and Ground Level Ozone in Europe – Part I: Unified EMEP Model Description, EMEP Status Report 2003, The Norwegian Meteorological Institute, Oslo, Norway, 2003.

Tesche, T. W., Morris, R., Tonnesen, G., McNally, D., Boylan, J., Brewer, P.: CMAQ/CAMx annual 2002 performance evaluation over the eastern United States, *Atmos. Environ.*, 40, 4906–4919, 2006.

Trainer, M., Parrish, D. D., Buhr, M. P., Norton, R. B., Fehsenfeld, F. C., Anlauf, K. G., Bottenheim, J. W., Tang, Y. Z., Wiebe, H. A., Roberts, J. M., Tanner, R. L., Newman, L., Bowersox, V. C., Meagher, J. F., Olszyna, K. J., Rodgers, M. O., Wang, T., Berresheim, H., Demerjian, K. L., and Roychowdhury, U. K.: Correlation of ozone with NO<sub>y</sub> in photochemically aged air, *J. Geophys. Res.-Atmos.*, 98, 2917–2925, 1993.

## Observations and modeling of air quality trends over 1990–2010 across the Northern Hemisphere

J. Xing et al.

Title Page

Abstract

Introduction

Conclusions

References

Tables

Figures

◀

▶

◀

▶

Back

Close

Full Screen / Esc

Printer-friendly Version

Interactive Discussion

- Tsimpidi, A. P., Karydis, V. A., and Pandis, S. N.: Response of inorganic fine particulate matter to emission changes of sulfur dioxide and ammonia: the Eastern United States as a case study, *JAPCA J. Air Waste Ma.*, 57, 1489–1498, doi:10.3155/1047-3289.57.12.1489, 2007.
- Wakamatsu, S., Morikawa, T., and Ito, A.: Air pollution trends in Japan between 1970 and 2012 and impact of urban air pollution countermeasures, *Asian Journal of Atmospheric Environment*, 7-4, 177–190, 2013.
- Wang, K., Zhang, Y., Jang, C., Phillips, S., and Wang, B.: Modeling intercontinental air pollution transport over the trans-Pacific region in 2001 using the Community Multiscale Air Quality modeling system, *J. Geophys. Res.-Atmos.*, 114, D04307, doi:10.1029/2008JD010807, 2009.
- Wang, S., Xing, J., Chatani, S., Hao, J., Klimont, Z., Cofala, J., and Amann, M.: Verification of anthropogenic emissions of China by satellite and ground observations, *Atmos. Environ.*, 45, 6347–6358, 2011a.
- Wang, S., Xing, J., Jang, C., Zhu, Y., Fu, J., and Hao, J.: Impact assessment of ammonia emissions on inorganic aerosols in east China using response surface modeling technique, *Environ. Sci. Technol.*, 45, 9293–9300, doi:10.1021/es2022347, 2011b.
- Wang, S., Xing, J., Zhao, B., Jang, C., and Hao, J.: Effectiveness of national air pollution control policies on the air quality in metropolitan areas of China, *J. Environ. Sci.*, 26, 13–22, 2014.
- Wang, Y., Konopka, P., Liu, Y., Chen, H., Müller, R., Plöger, F., Riese, M., Cai, Z., and Lü, D.: Tropospheric ozone trend over Beijing from 2002–2010: ozonesonde measurements and modeling analysis, *Atmos. Chem. Phys.*, 12, 8389–8399, doi:10.5194/acp-12-8389-2012, 2012.
- Wild, M.: Global dimming and brightening: a review, *J. Geophys. Res.*, 114, D00D16, doi:10.1029/2008JD011470, 2009.
- Xing, J., Zhang, Y., Wang, S., Liu, X., Cheng, S., Zhang, Q., Chen, Y., Hao, J., and Wang, W.: Modeling study on the air quality impacts from emission reductions and atypical meteorological conditions during the 2008 Beijing Olympics, *Atmos. Environ.*, 45, 1786–1798, 2011a.
- Xing, J., Wang, S. X., Jang, C., Zhu, Y., and Hao, J. M.: Nonlinear response of ozone to precursor emission changes in China: a modeling study using response surface methodology, *Atmos. Chem. Phys.*, 11, 5027–5044, doi:10.5194/acp-11-5027-2011, 2011b.
- Xing, J., Pleim, J., Mathur, R., Pouliot, G., Hogrefe, C., Gan, C.-M., and Wei, C.: Historical gaseous and primary aerosol emissions in the United States from 1990 to 2010, *Atmos. Chem. Phys.*, 13, 7531–7549, doi:10.5194/acp-13-7531-2013, 2013.

## Observations and modeling of air quality trends over 1990–2010 across the Northern Hemisphere

J. Xing et al.

Title Page

Abstract

Introduction

Conclusions

References

Tables

Figures

◀

▶

◀

▶

Back

Close

Full Screen / Esc

Printer-friendly Version

Interactive Discussion



Xiu, A. and Pleim, J. E.: Development of a land surface model. Part I: Application in a mesoscale meteorological model, *J. Appl. Meteorol.*, 40, 192–209, 2001.

Xu, X. and Lin, W.: Trends of tropospheric ozone over china based on satellite data (1979–2005), *Advances in Climate Change Research*, 2, 43–48, 2011.

5 Yamaji, K., Ohara, T., Uno, I., Tanimoto, H., Kurokawa, J. I., and Akimoto, H.: Analysis of the seasonal variation of ozone in the boundary layer in East Asia using the Community Multi-scale Air Quality model: what controls surface ozone levels over Japan?, *Atmos. Environ.*, 40, 1856–1868, 2006.

10 Zhang, H., Chen, G., Hu, J., Chen, S.-H., Wiedinmyer, C., Kleeman, M., and Ying, Q.: Evaluation of a seven-year air quality simulation using the Weather Research and Forecasting (WRF)/Community Multiscale Air Quality (CMAQ) models in the eastern United States, *Sci. Total Environ.*, 473–474, 275–285, 2014.

Zhang, X., Zhang, P., Zhang, Y., Li, X., and Qiu, H.: The trend, seasonal cycle, and sources of tropospheric NO<sub>2</sub> over China during 1997–2006 based on satellite measurement, *Sci. China Ser. D*, 50, 1877–1884, 2007.

15 Zhang, X., van Geffen, J., Liao, H., Zhang, P., and Lou, S. J.: Spatiotemporal variations of tropospheric SO<sub>2</sub> over China by SCIAMACHY observations during 2004–2009, *Atmos. Environ.*, 60, 238–246, 2012.

20 Zhang, Y., Vijayaraghavan, K., Wen, X.-Y., Snell, H. E., and Jacobson, M. Z.: Probing into regional ozone and particulate matter pollution in the United States: 1. A 1 year CMAQ simulation and evaluation using surface and satellite data, *J. Geophys. Res.*, 114, D22304, doi:10.1029/2009JD011898, 2009.

25 Zhao, B., Wang, S. X., Dong, X. Y., Wang, J. D., Duan, L., Fu, X., Hao, J., and Fu, J.: Environmental effects of the recent emission changes in China: implications for particulate matter pollution and soil acidification, *Environ. Res. Lett.*, 8, 24031, doi:10.1088/1748-9326/8/2/024031, 2013.



**Table 2a.** Model performance: gaseous species.

Species	Network	Obs ( $\mu\text{g m}^{-3}$ )	<i>R</i>	MB ( $\mu\text{g m}^{-3}$ )	NMB (%)	RMSE ( $\mu\text{g m}^{-3}$ )	NME (%)	<i>N</i> pairs		
SO <sub>2</sub>	US-CASTNET	Spring	5.0	0.73	-1.1	-21.8	3.2	72.4	2316	
		Summer	3.3	0.74	0.2	5.3	2.4	93.4	2352	
		Fall	4.5	0.78	1.6	36.0	3.8	118.0	2348	
		Winter	8.1	0.67	-2.7	-33.4	6.0	81.7	2317	
		Annual	5.2	0.67	-0.5	-9.4	4.1	91.5	9333	
	US-AQS	Annual	14.0	0.5	-6.4	-46.1	11.2	98.2	5563	
	EU- AIRBASE	Annual	8.3	0.52	-1.0	-11.8	6.5	58.4	2343	
	EU-EMEP	Spring	2.4	0.43	2.0	82.2	5.0	239.8	2399	
		Summer	1.6	0.44	2.4	150.1	4.7	325.0	2355	
		Fall	2.2	0.48	2.2	102.7	4.9	324.1	2344	
Winter		3.8	0.50	0.1	3.6	5.2	177.6	2363		
Annual		2.5	0.43	1.7	67.0	5.0	266.3	9461		
CN-API	Annual	50.8	0.33	-18.4	-36.3	28.4	42.2	42		
NO <sub>2</sub>	US-AQS	Annual	33.1	0.6	-17.9	-54.1	23.6	58.7	3612	
	EU- AIRBASE	Annual	30.9	0.18	-17.7	-57.3	23.1	57.2	3049	
	EU-EMEP	Spring	6.5	0.65	-0.1	-1.6	5.6	79.5	2049	
		Summer	5.0	0.56	-0.7	-14.1	4.7	73.8	2066	
		Fall	7.1	0.67	1.0	14.4	7.0	84.1	2084	
		Winter	9.7	0.68	1.3	13.9	7.9	91.6	2068	
		Annual	7.1	0.68	0.4	5.6	6.4	82.3	8267	
	CN-API	Annual	46.6	0.08	-31.5	-67.5	36.1	66.2	42	
	O <sub>3</sub> *	US-CASTNET	Spring	168.1	0.52	-22.8	-13.6	29.7	16.1	1269
			Summer	176.8	0.59	-14.3	-8.1	30.5	14.5	1512
Fall			155.3	0.60	-3.9	-2.5	23.5	12.4	1071	
Winter			112.5	0.51	-3.6	-3.2	10.1	7.6	217	
EU-AIRBASE		Annual	169.4	0.40	14.4	8.5	38.9	17.4	2776	
EU-EMEP		Spring	140.9	0.56	-2.1	-1.5	22.7	14.2	4145	
		Summer	152.3	0.60	6.5	4.3	30.5	18.4	4161	
		Fall	108.5	0.66	18.4	16.9	25.4	25.9	4151	
		Winter	92.5	0.29	3.1	3.4	16.1	16.6	4111	
WDCGG-JP		Spring	165.4	0.68	-8.9	-5.4	26.1	14.4	175	
	Summer	157.3	0.83	10.8	6.9	34.0	21.4	172		
	Fall	128.5	0.62	17.4	13.5	31.4	21.9	173		
	Winter	109.2	0.49	3.2	2.9	15.1	12.6	172		

\* Comparison of O<sub>3</sub> concentration is computed on the basis of annual or seasonal maximum of DM8 (daily 8 h maxima) value, except that for AIRBASE which is computed on the basis of annual maxima of DM1 (daily 1 h maxima).

**Table 2b.** Model performance: fine particles.

Species	Network	Obs ( $\mu\text{g m}^{-3}$ )	<i>R</i>	MB ( $\mu\text{g m}^{-3}$ )	NMB (%)	RMSE ( $\mu\text{g m}^{-3}$ )	NME (%)	<i>N</i> pairs		
$\text{SO}_4^{2-}$	US-CASTNET	Spring	3.1	0.87	-0.2	-7.5	0.8	29.2	2316	
		Summer	5.3	0.86	-2.4	-45.2	3.1	44.7	2352	
		Fall	3.7	0.86	-1.0	-26.5	1.8	34.3	2348	
		Winter	2.3	0.63	-0.8	-35.6	1.2	53.1	2316	
		Annual	3.6	0.81	-1.1	-30.8	1.9	40.3	9332	
	US-IMPROVE	Spring	1.4	0.89	0.3	22.5	0.7	70.3	1602	
		Summer	2.2	0.90	-0.6	-28.9	1.8	37.8	1596	
		Fall	1.3	0.90	0.2	15.7	0.7	68.4	1605	
		Winter	0.9	0.76	0.1	16.3	0.6	106.7	1605	
		Annual	1.4	0.85	0.0	0.7	1.1	70.8	6408	
	EU-EMEP	Spring	2.6	0.68	0.3	12.5	1.4	52.3	2099	
		Summer	2.4	0.68	0.1	3.7	1.3	41.4	2071	
		Fall	2.2	0.64	0.0	1.9	1.4	55.9	2042	
		Winter	2.4	0.53	-0.7	-28.6	1.9	58.3	2058	
		Annual	2.4	0.61	-0.1	-2.4	1.5	51.9	8270	
$\text{NO}_3^-$	US-CASTNET	Spring	1.1	0.69	1.0	92.9	2.1	195.5	2316	
		Summer	0.4	0.31	-0.2	-48.2	0.4	76.1	2352	
		Fall	0.7	0.68	0.1	13.8	0.7	99.3	2348	
		Winter	1.6	0.71	1.2	75.2	1.9	262.0	2316	
		Annual	0.9	0.72	0.5	56.4	1.5	157.7	9332	
	US-IMPROVE	Spring	0.4	0.72	0.4	106.9	1.0	164.8	1602	
		Summer	0.2	0.10	-0.1	-40.5	0.2	93.0	1596	
		Fall	0.3	0.66	0.0	11.4	0.4	125.7	1604	
		Winter	0.5	0.66	0.5	94.8	1.1	226.9	1605	
		Annual	0.3	0.66	0.2	59.1	0.8	152.7	6407	
	EU-EMEP	Spring	3.0	0.75	0.3	10.8	2.0	75.2	679	
		Summer	1.8	0.74	-1.2	-67.0	1.5	74.7	656	
		Fall	2.3	0.72	-0.4	-15.0	1.5	64.4	659	
		Winter	2.6	0.64	0.6	23.1	2.1	91.2	671	
		Annual	2.4	0.70	-0.2	-6.3	1.8	76.4	2665	
$\text{NH}_4^+$	US-CASTNET	Spring	1.2	0.68	0.3	22.6	0.8	52.0	2316	
		Summer	1.6	0.77	-0.8	-53.7	1.1	50.5	2352	
		Fall	1.2	0.72	-0.3	-21.4	0.6	31.7	2348	
		Winter	1.1	0.76	0.2	19.0	0.6	54.1	2316	
		Annual	1.3	0.52	-0.2	-12.9	0.8	47.0	9332	
	EU-EMEP	Spring	1.4	0.69	0.7	51.3	1.4	101.4	335	
		Summer	1.2	0.64	-0.2	-15.2	0.9	43.9	330	
		Fall	1.2	0.67	0.3	28.2	1.0	73.7	332	
		Winter	1.1	0.62	0.8	68.4	1.4	110.4	328	
		Annual	1.2	0.62	0.4	33.7	1.2	82.4	1325	
	EC	US-IMPROVE	Spring	0.2	0.79	-0.1	-62.5	0.2	62.7	1536
			Summer	0.3	0.54	-0.2	-73.5	0.3	92.7	1532
			Fall	0.3	0.81	-0.2	-64.4	0.3	65.9	1548
			Winter	0.2	0.85	-0.1	-59.4	0.2	55.7	1542
			Annual	0.2	0.74	-0.2	-65.1	0.3	69.2	6158

\* Comparison of  $\text{O}_3$  concentration is computed on the basis of annual or seasonal maximum of DM8 (daily 8h maxima) value, except that for AIRBASE which is computed on the basis of annual maxima of DM1 (daily 1h maxima).

## Observations and modeling of air quality trends over 1990–2010 across the Northern Hemisphere

J. Xing et al.

**Table 3.** Simulated trends in three regions (grid-averaged).

	Eastern China %		Eastern US %		Europe %	
Emission ( $\text{kg km}^{-2} \text{yr}^{-1}$ )						
SO <sub>2</sub>	<b>20.2</b>	<b>3.2</b>	<i>-16.1</i>	<i>-5.4</i>	<i>-20.4</i>	<i>-5.4</i>
NO <sub>x</sub>	<b>8.5</b>	<b>4.3</b>	<i>-3.7</i>	<i>-1.8</i>	<i>-3.0</i>	<i>-1.5</i>
VOC	<b>18.6</b>	<b>2.3</b>	<i>-22.5</i>	<i>-3.3</i>	<i>-26.7</i>	<i>-3.3</i>
NH <sub>3</sub>	<b>6.5</b>	<b>2.6</b>	<b>1.7</b>	<b>1.6</b>	<i>-2.6</i>	<i>-1.0</i>
PM <sub>10</sub>	2.1	0.3	<i>-4.5</i>	<i>-4.6</i>	<i>-10.0</i>	<i>-4.8</i>
Concentration ( $\mu\text{g m}^{-3} \text{yr}^{-1}$ )						
SO <sub>2</sub>	<b>0.265</b>	<b>2.70</b>	<i>-0.175</i>	<i>-5.71</i>	<i>-0.178</i>	<i>-5.06</i>
NO <sub>2</sub>	<b>0.119</b>	<b>4.14</b>	<i>-0.048</i>	<i>-1.38</i>	<i>-0.040</i>	<i>-1.16</i>
*O <sub>3</sub>	<b>2.566</b>	<b>1.49</b>	<i>-1.028</i>	<i>-0.66</i>	<i>-0.875</i>	<i>-0.54</i>
PM <sub>2.5</sub>	<b>0.481</b>	<b>2.21</b>	<i>-0.097</i>	<i>-1.21</i>	<i>-0.253</i>	<i>-2.62</i>
SO <sub>4</sub> <sup>2-</sup>	<b>0.185</b>	<b>2.82</b>	<i>-0.072</i>	<i>-3.17</i>	<i>-0.109</i>	<i>-3.73</i>
NO <sub>3</sub> <sup>-</sup>	<b>0.097</b>	<b>5.40</b>	<b>0.014</b>	<b>1.61</b>	<i>-0.030</i>	<i>-1.84</i>
NH <sub>4</sub> <sup>+</sup>	<b>0.081</b>	<b>3.44</b>	<i>-0.006</i>	<i>-0.72</i>	<i>-0.041</i>	<i>-2.91</i>
EC	<b>0.005</b>	<b>0.99</b>	<i>-0.004</i>	<i>-3.39</i>	<i>-0.005</i>	<i>-2.46</i>

Formatted entries are significant at  $p = 0.05$  level: italic = significant decrease; bold = significant increase.

\* Trend in O<sub>3</sub> is computed on the basis of annual or seasonal maximum of DM8 (daily 8 h maxima) value.

[Title Page](#)
[Abstract](#)
[Introduction](#)
[Conclusions](#)
[References](#)
[Tables](#)
[Figures](#)
[◀](#)
[▶](#)
[◀](#)
[▶](#)
[Back](#)
[Close](#)
[Full Screen / Esc](#)
[Printer-friendly Version](#)
[Interactive Discussion](#)


## Observations and modeling of air quality trends over 1990–2010 across the Northern Hemisphere

J. Xing et al.

**Table 4.** Comparison of observed and simulated trend (unit:  $\mu\text{g m}^{-3}\text{ yr}^{-1}$ , computed on the basis of annual and seasonal means over the 1990–2010 period with a linear least square fit method) and the annual change rate ( $x\%$ , i.e., concentration in the year  $Y$  ( $C_Y$ ) will be fit as  $C_Y = C_{1990} \times (1 + x)^{Y-1990}$ ).

Species	Network		Spring		Summer		Fall		Winter		Annual	
			obs	sim								
SO <sub>2</sub>	US-CASTNET	$\mu\text{g m}^{-3}$	<i>-0.228</i>	<i>-0.238</i>	<i>-0.152</i>	<i>-0.204</i>	<i>-0.234</i>	<i>-0.385</i>	<i>-0.368</i>	<i>-0.366</i>	<i>-0.245</i>	<i>-0.298</i>
		%	<i>-4.74</i>	<i>-6.26</i>	<i>-4.91</i>	<i>-6.13</i>	<i>-5.61</i>	<i>-6.63</i>	<i>-4.79</i>	<i>-7.01</i>	<i>-4.98</i>	<i>-6.57</i>
	US-AQS	$\mu\text{g m}^{-3}$									<i>-0.755</i>	<i>-0.439</i>
		%									<i>-5.5</i>	<i>-6.0</i>
	EU-AIRBASE	$\mu\text{g m}^{-3}$									<i>-0.763</i>	<i>-0.515</i>
%										<i>-8.65</i>	<i>-6.55</i>	
EU-EMEP	$\mu\text{g m}^{-3}$	<i>-0.187</i>	<i>-0.282</i>	<i>-0.108</i>	<i>-0.225</i>	<i>-0.180</i>	<i>-0.279</i>	<i>-0.339</i>	<i>-0.264</i>	<i>-0.204</i>	<i>-0.262</i>	
	%	<i>-7.03</i>	<i>-6.16</i>	<i>-5.95</i>	<i>-5.53</i>	<i>-7.28</i>	<i>-6.23</i>	<i>-8.04</i>	<i>-6.28</i>	<i>-7.26</i>	<i>-6.05</i>	
CN-API	$\mu\text{g m}^{-3}$									0.376	1.230	
	%									0.66	4.02	
NO <sub>2</sub>	US-AQS	$\mu\text{g m}^{-3}$								<i>-0.911</i>	<i>-0.358</i>	
		%								<i>-2.8</i>	<i>-2.4</i>	
	EU-AIRBASE	$\mu\text{g m}^{-3}$								<i>-0.592</i>	<i>-0.220</i>	
		%								<i>-1.83</i>	<i>-1.58</i>	
	EU-EMEP	$\mu\text{g m}^{-3}$	<i>-0.087</i>	<i>-0.113</i>	<i>-0.115</i>	<i>-0.137</i>	<i>-0.150</i>	<i>-0.194</i>	<i>-0.150</i>	<i>-0.195</i>	<i>-0.126</i>	<i>-0.160</i>
%		<i>-1.29</i>	<i>-1.64</i>	<i>-2.26</i>	<i>-3.03</i>	<i>-2.00</i>	<i>-2.30</i>	<i>-1.46</i>	<i>-1.70</i>	<i>-1.69</i>	<i>-2.04</i>	
CN-API	$\mu\text{g m}^{-3}$									<i>-0.454</i>	<b>0.868</b>	
	%									<i>-0.97</i>	<b>5.94</b>	
O <sub>3</sub> *	US-CASTNET	$\mu\text{g m}^{-3}$	<i>-1.187</i>	<i>-0.903</i>	<i>-1.860</i>	<i>-1.010</i>	<i>-1.220</i>	<i>-0.527</i>	<i>-0.029</i>	<i>-0.134</i>	<i>-1.859</i>	<i>-0.952</i>
		%	<i>-0.73</i>	<i>-0.65</i>	<i>-1.14</i>	<i>-0.68</i>	<i>-0.83</i>	<i>-0.36</i>	<i>-0.02</i>	<i>-0.13</i>	<i>-1.10</i>	<i>-0.64</i>
	EU-AIRBASE	$\mu\text{g m}^{-3}$									<i>-1.348</i>	<i>-2.129</i>
		%									<i>-0.79</i>	<i>-1.13</i>
	EU-EMEP	$\mu\text{g m}^{-3}$	<i>-0.651</i>	<i>-1.281</i>	<i>-1.207</i>	<i>-1.365</i>	<i>-0.157</i>	<i>-0.184</i>	0.124	<i>-0.048</i>	<i>-1.067</i>	<i>-1.313</i>
		%	<i>-0.46</i>	<i>-0.92</i>	<i>-0.85</i>	<i>-0.91</i>	<i>-0.13</i>	<i>-0.15</i>	0.14	<i>-0.05</i>	<i>-0.74</i>	<i>-0.87</i>
	WDCGG-Minamitorishima	$\mu\text{g m}^{-3}$	0.485	<i>-0.029</i>	<i>-1.131</i>	<i>-0.083</i>	<i>-0.688</i>	0.090	<i>-0.416</i>	0.413	0.232	<i>-0.126</i>
		%	0.35	<i>-0.02</i>	<i>-1.19</i>	0.01	<i>-0.70</i>	0.09	<i>-0.31</i>	0.38	0.18	<i>-0.11</i>
WDCGG-Ryori	$\mu\text{g m}^{-3}$	1.305	0.372	0.549	0.259	<i>-0.638</i>	0.308	0.166	0.217	0.702	0.440	
	%	0.79	0.24	0.44	0.18	<i>-0.47</i>	0.25	0.24	0.23	0.41	0.29	
WDCGG-Tsukuba	$\mu\text{g m}^{-3}$	<i>-1.073</i>	<i>-0.019</i>	<i>-4.015</i>	<i>-0.375</i>	0.581	<i>-1.017</i>	<i>-0.368</i>	<b>0.861</b>	<i>-3.299</i>	<i>-0.022</i>	
	%	<i>-0.60</i>	<i>-0.02</i>	<i>-1.78</i>	<i>-0.18</i>	0.52	<i>-0.56</i>	<i>-0.31</i>	<b>0.74</b>	<i>-1.40</i>	<i>-0.01</i>	

Formatted entries are significant at  $p = 0.05$  level; italic = significant decrease; bold = significant increase.

\* Trend in O<sub>3</sub> is computed on the basis of annual or seasonal maximum of DM8 (daily 8 h maxima) value, except that for AIRBASE which is computed on the basis of annual maximum of DM1 (daily 1 h maxima).

Title Page

Abstract

Introduction

Conclusions

References

Tables

Figures

◀

▶

◀

▶

Back

Close

Full Screen / Esc

Printer-friendly Version

Interactive Discussion

## Observations and modeling of air quality trends over 1990–2010 across the Northern Hemisphere

J. Xing et al.

**Table 4.** Continued.

Species	Network		Spring		Summer		Fall		Winter		Annual	
			obs	sim								
SO <sub>4</sub> <sup>2-</sup>	US-CASTNET	μg m <sup>-3</sup>	-0.070	-0.073	-0.161	-0.125	-0.112	-0.098	-0.054	-0.046	-0.099	-0.086
		%	-2.30	-2.49	-3.25	-4.45	-3.31	-3.75	-2.25	-3.01	-2.87	-3.46
	US-IMPROVE	μg m <sup>-3</sup>	-0.023	-0.021	-0.049	-0.043	-0.036	-0.041	-0.024	-0.016	-0.033	-0.030
		%	-1.76	-1.24	-2.45	-2.86	-2.87	-2.69	-2.76	-1.59	-2.43	-2.11
	EU-EMEP	μg m <sup>-3</sup>	-0.119	-0.086	-0.111	-0.112	-0.097	-0.085	-0.090	-0.060	-0.104	-0.086
		%	-4.28	-2.84	-4.35	-4.49	-4.27	-3.93	-3.39	-3.29	-4.06	-3.62
NO <sub>3</sub> <sup>-</sup>	US-CASTNET	μg m <sup>-3</sup>	-0.009	0.023	-0.011	<b>0.005</b>	-0.015	<b>0.023</b>	0.009	<b>0.057</b>	-0.006	<b>0.027</b>
		%	-0.94	1.19	-3.17	<b>3.38</b>	-2.27	<b>3.33</b>	0.61	<b>2.35</b>	-0.73	<b>2.10</b>
	US-IMPROVE	μg m <sup>-3</sup>	-0.002	<b>0.012</b>	-0.004	0.000	-0.005	<b>0.010</b>	-0.002	<b>0.024</b>	-0.003	<b>0.012</b>
		%	-0.70	<b>1.93</b>	-2.13	0.14	-1.97	<b>3.73</b>	-0.28	<b>2.99</b>	-1.04	<b>2.53</b>
	EU-EMEP	μg m <sup>-3</sup>	-0.015	-0.086	-0.019	-0.032	-0.009	-0.043	0.013	-0.002	-0.008	-0.041
		%	-0.47	-2.49	-1.06	-5.38	-0.51	-2.19	0.50	-0.13	-0.33	-1.74
NH <sub>4</sub> <sup>+</sup>	US-CASTNET	μg m <sup>-3</sup>	-0.023	-0.002	-0.038	-0.010	-0.032	-0.006	-0.013	<b>0.012</b>	-0.026	-0.002
		%	-2.04	-0.19	-2.60	-1.54	-2.86	-0.68	-1.24	<b>0.97</b>	-2.19	-0.18
	EU-EMEP	μg m <sup>-3</sup>	0.003	-0.055	0.000	-0.049	0.020	-0.035	-0.002	-0.018	0.005	-0.039
		%	0.80	-2.22	0.30	-4.52	1.75	-2.21	0.16	-0.87	0.70	-2.19
EC	US-IMPROVE	μg m <sup>-3</sup>	-0.005	-0.002	-0.003	-0.002	-0.009	-0.004	-0.008	-0.003	-0.006	-0.003
		%	-2.46	-2.77	-1.34	-3.42	-3.30	-3.67	-3.41	-3.32	-2.64	-3.32

Formatted entries are significant at  $p = 0.05$  level: italic = significant decrease; bold = significant increase.

\* Trend in O<sub>3</sub> is computed on the basis of annual or seasonal maximum of DM8 (daily 8 h maxima) value, except that for AIRBASE which is computed on the basis of annual maximum of DM1 (daily 1 h maxima).

Title Page

Abstract Introduction

Conclusions References

Tables Figures

◀ ▶

◀ ▶

Back Close

Full Screen / Esc

Printer-friendly Version

Interactive Discussion



**Observations and modeling of air quality trends over 1990–2010 across the Northern Hemisphere**

J. Xing et al.

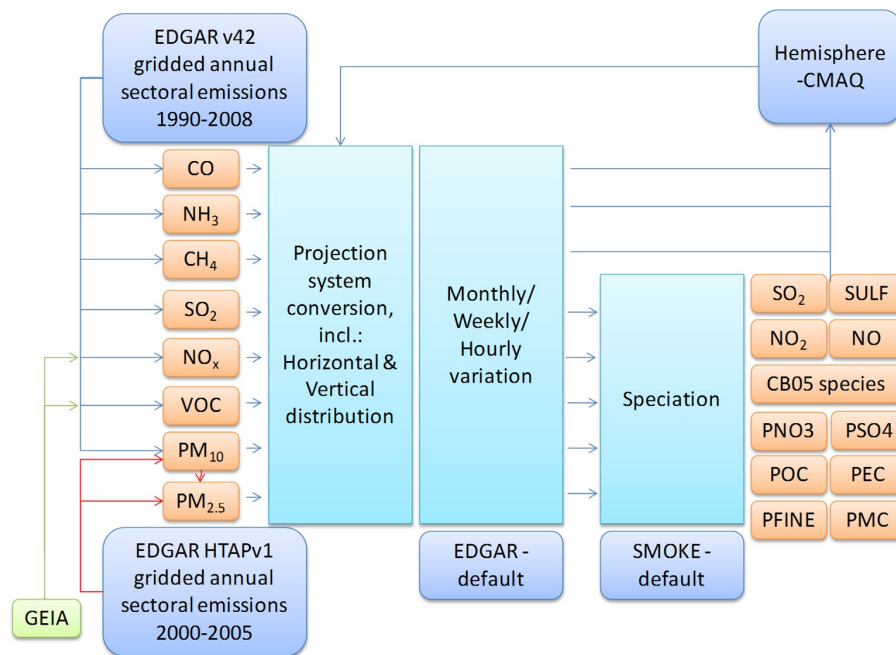


**Figure 1.** Processes of gridded emissions for northern hemispheric WRF-CMAQ simulation.

Title Page	
Abstract	Introduction
Conclusions	References
Tables	Figures
◀	▶
◀	▶
Back	Close
Full Screen / Esc	
Printer-friendly Version	
Interactive Discussion	



## Observations and modeling of air quality trends over 1990–2010 across the Northern Hemisphere

J. Xing et al.

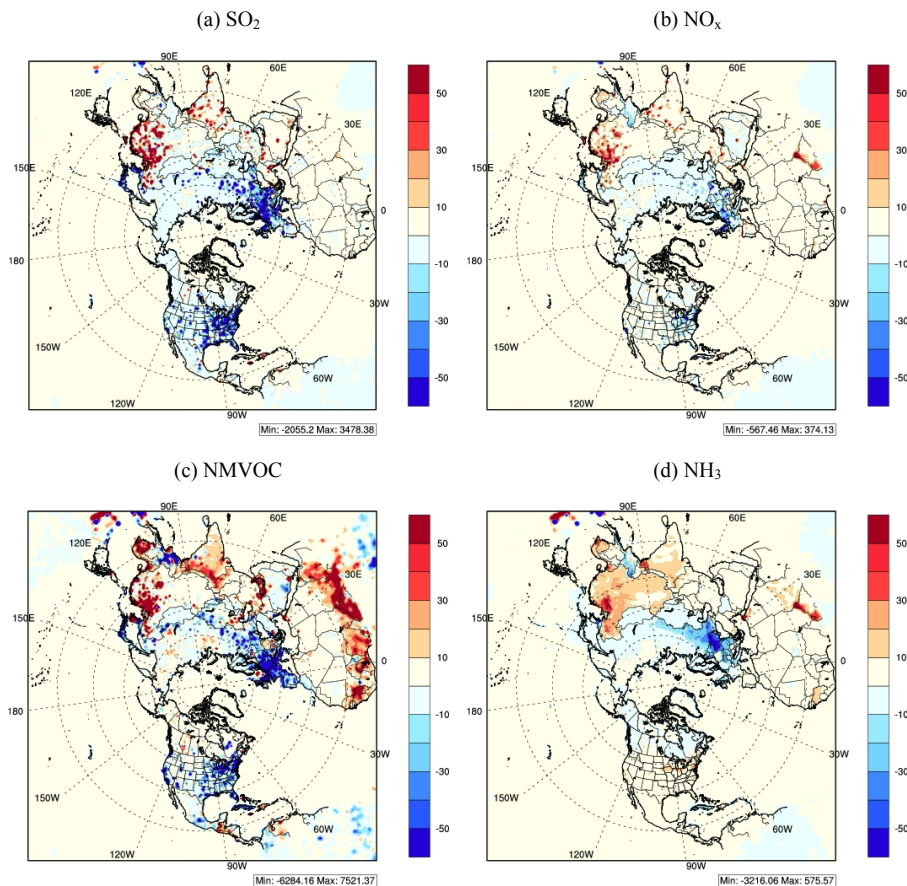


**Figure 2.** EDGAR emission trend over 1990 to 2010 for SO<sub>2</sub>, NO<sub>x</sub>, NMVOC and NH<sub>3</sub> (unit: kg km<sup>-2</sup> yr<sup>-1</sup>, computed on the basis of annual means over the 1990–2010 period with a linear least square fit method).

## Observations and modeling of air quality trends over 1990–2010 across the Northern Hemisphere

J. Xing et al.

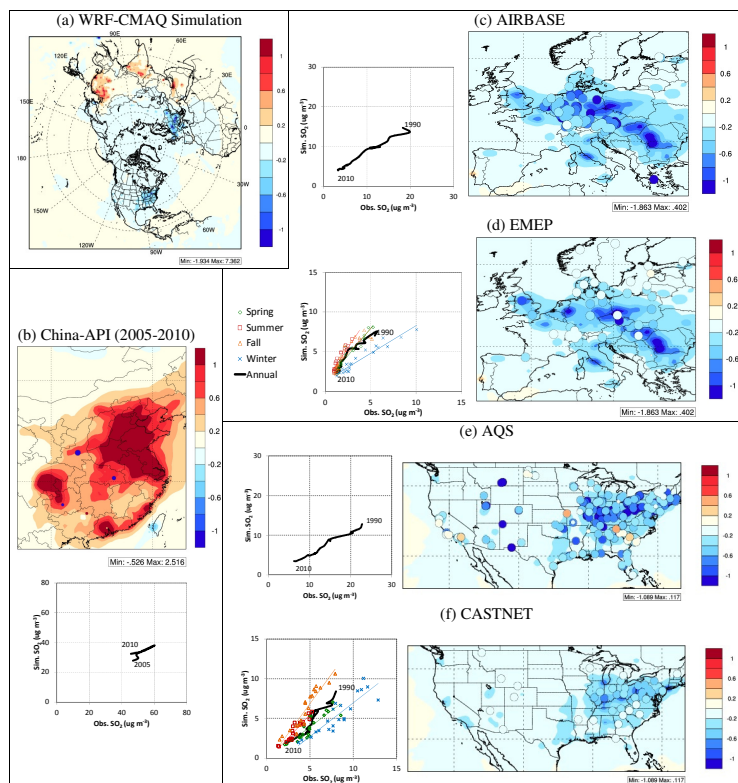


**Figure 3.** Observed and simulated SO<sub>2</sub> concentration (scatter plot, unit:  $\mu\text{g m}^{-3}$ , network-mean for each year or season, corresponding grids from model simulation are selected for comparison) and trend (color map, unit:  $\mu\text{g m}^{-3} \text{ yr}^{-1}$ , dot represents each observation site, computed on the basis of annual means over the 1990–2010 period with a linear least square fit method; dot size is determined by the significance of trend, i.e., larger symbols denote more significant trends at 0.05 level).

## Observations and modeling of air quality trends over 1990–2010 across the Northern Hemisphere

J. Xing et al.

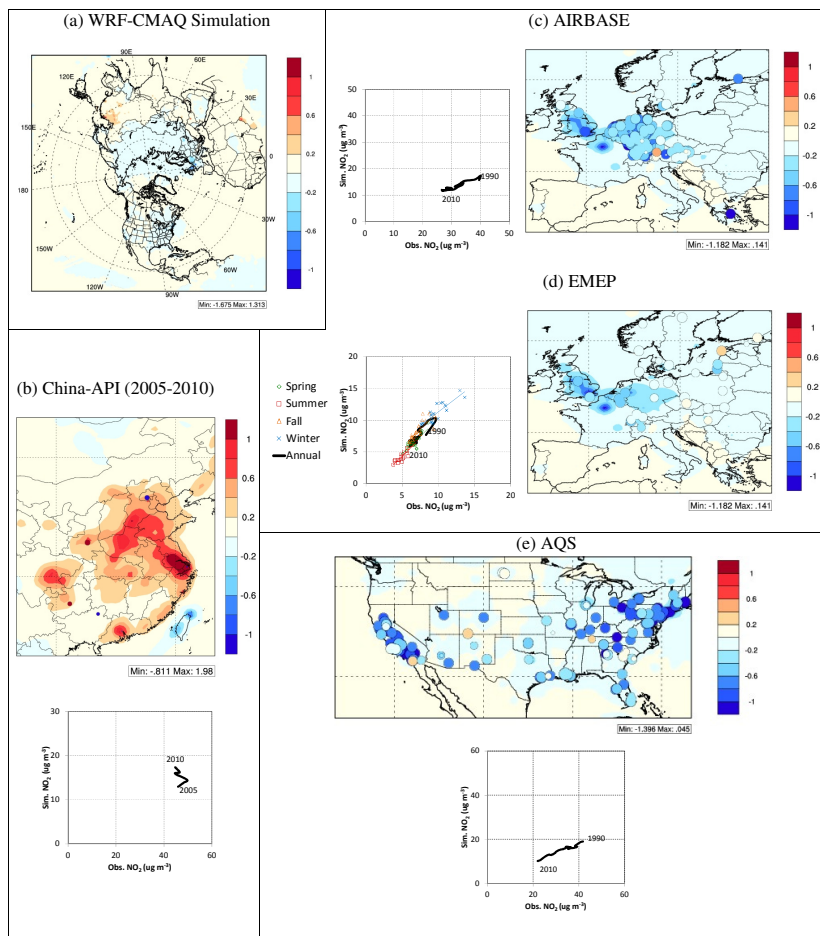


**Figure 4.** Same as Fig. 3 for  $\text{NO}_2$ .

Observations and modeling of air quality trends over 1990–2010 across the Northern Hemisphere

J. Xing et al.

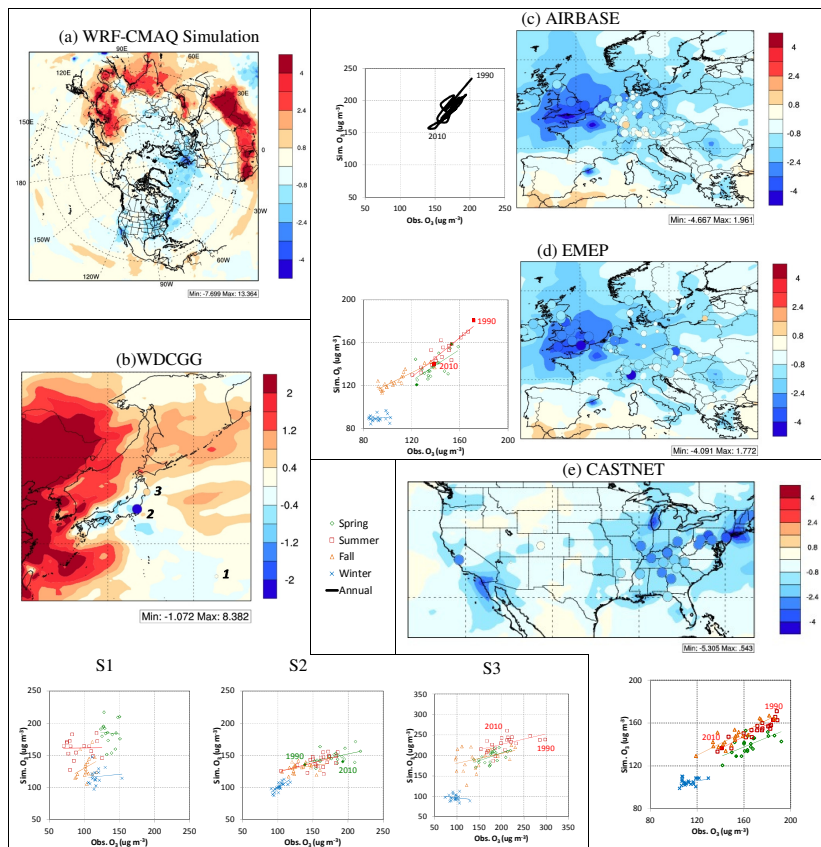


**Figure 5.** Same as Fig. 3 for  $O_3$  (unit:  $\mu\text{g m}^{-3}$ , computed on the basis of annual or seasonal maximum of DM8 (daily 8 h maxima) value, except that for AIRBASE which is computed on the basis of annual maximum of DM1 (daily 1 h maxima); three sites of WDCGG are S1 – Minamitorishima, lat: 24.28, lon: 153.98, S2 – Ryori, lat: 39.03, lon: 141.82, S3 – Tsukuba, lat: 36.05, lon: 140.13).

Title Page

Abstract Introduction

Conclusions References

Tables Figures

◀ ▶

◀ ▶

Back Close

Full Screen / Esc

Printer-friendly Version

Interactive Discussion

Observations and modeling of air quality trends over 1990–2010 across the Northern Hemisphere

J. Xing et al.

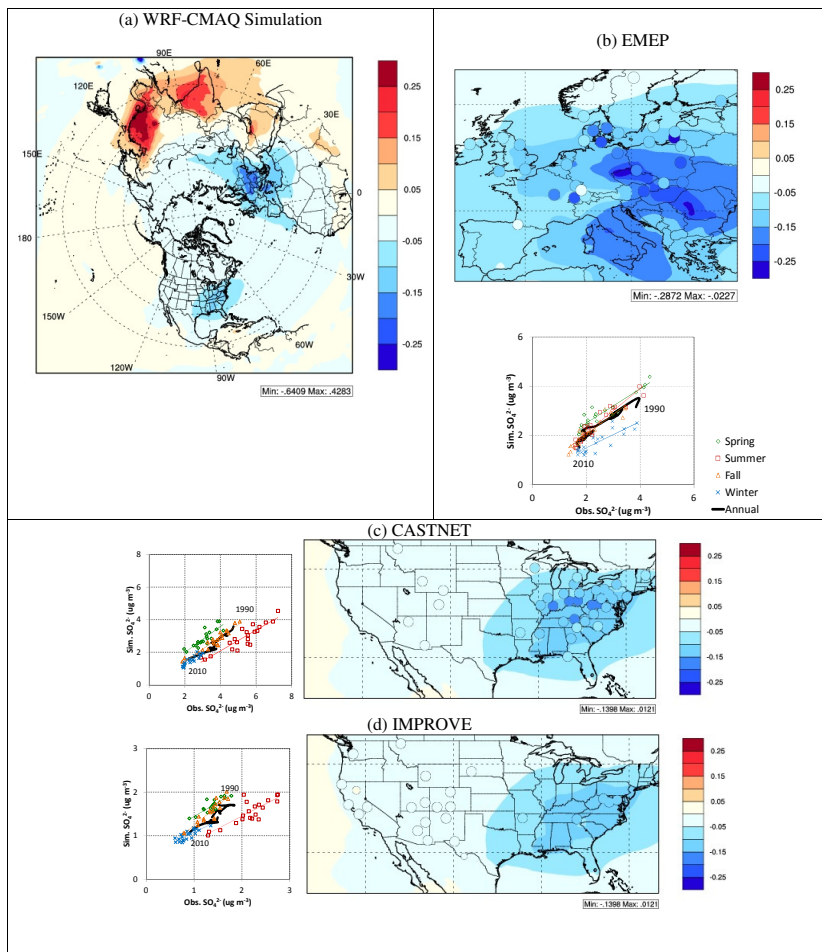


Figure 6. Same as Fig. 3 for  $\text{SO}_4^{2-}$ .

Title Page

Abstract Introduction

Conclusions References

Tables Figures

◀ ▶

◀ ▶

Back Close

Full Screen / Esc

Printer-friendly Version

Interactive Discussion

Observations and modeling of air quality trends over 1990–2010 across the Northern Hemisphere

J. Xing et al.

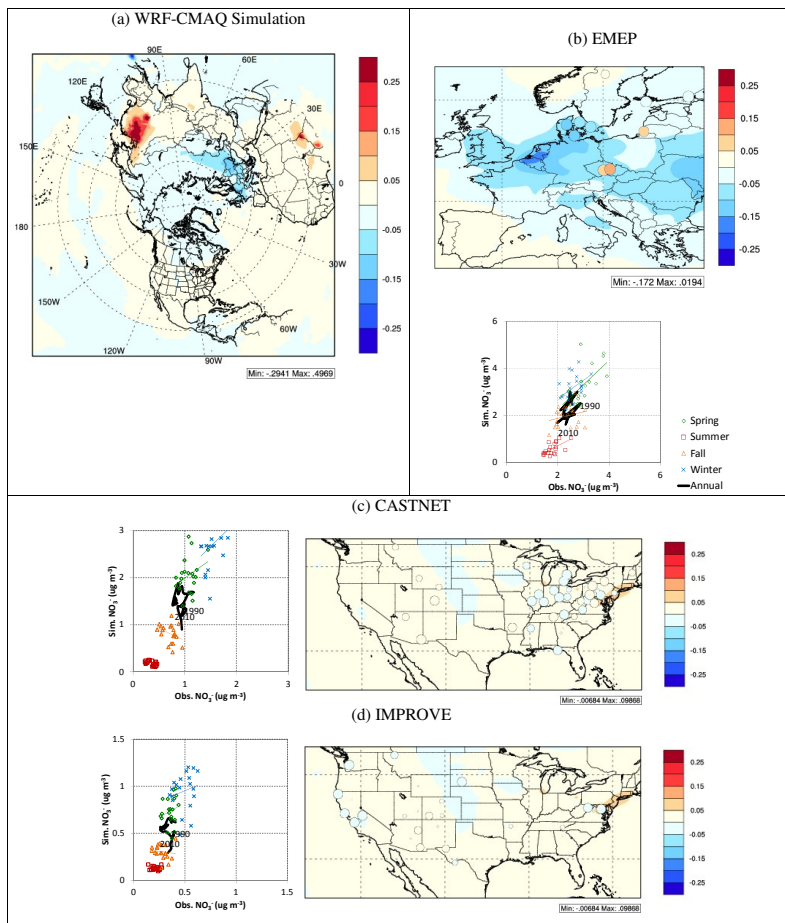


Figure 7. Same as Fig. 3 for  $\text{NO}_3^-$ .

Title Page

Abstract Introduction

Conclusions References

Tables Figures

◀ ▶

◀ ▶

Back Close

Full Screen / Esc

Printer-friendly Version

Interactive Discussion

## Observations and modeling of air quality trends over 1990–2010 across the Northern Hemisphere

J. Xing et al.

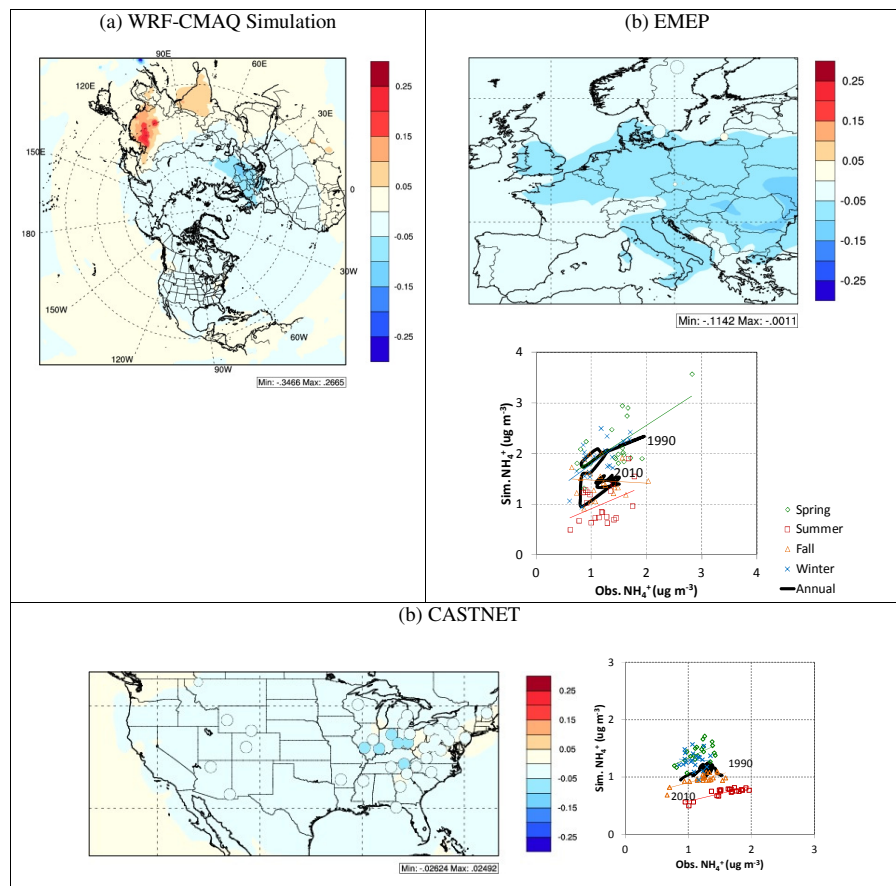


**Figure 8.** Same as Fig. 3 for  $\text{NH}_4^+$ .

Observations and modeling of air quality trends over 1990–2010 across the Northern Hemisphere

J. Xing et al.

Title Page

Abstract

Introduction

Conclusions

References

Tables

Figures

◀

▶

◀

▶

Back

Close

Full Screen / Esc

Printer-friendly Version

Interactive Discussion

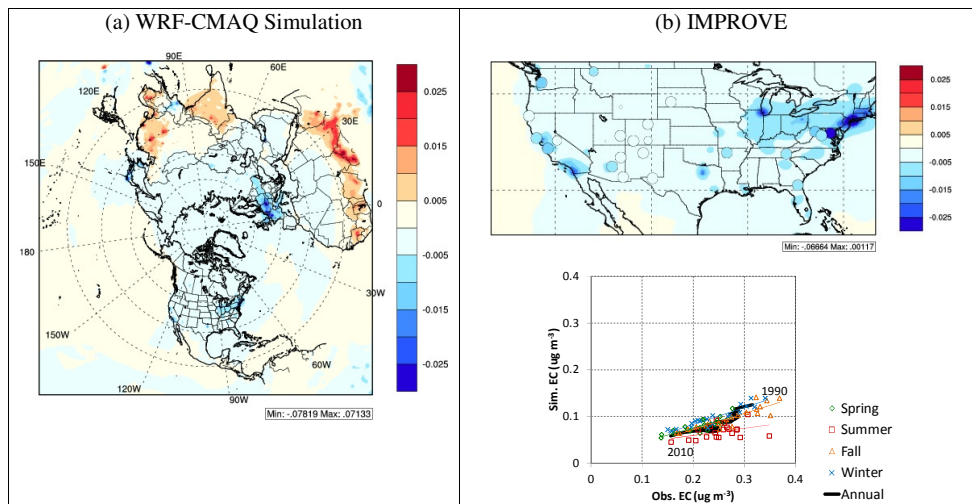
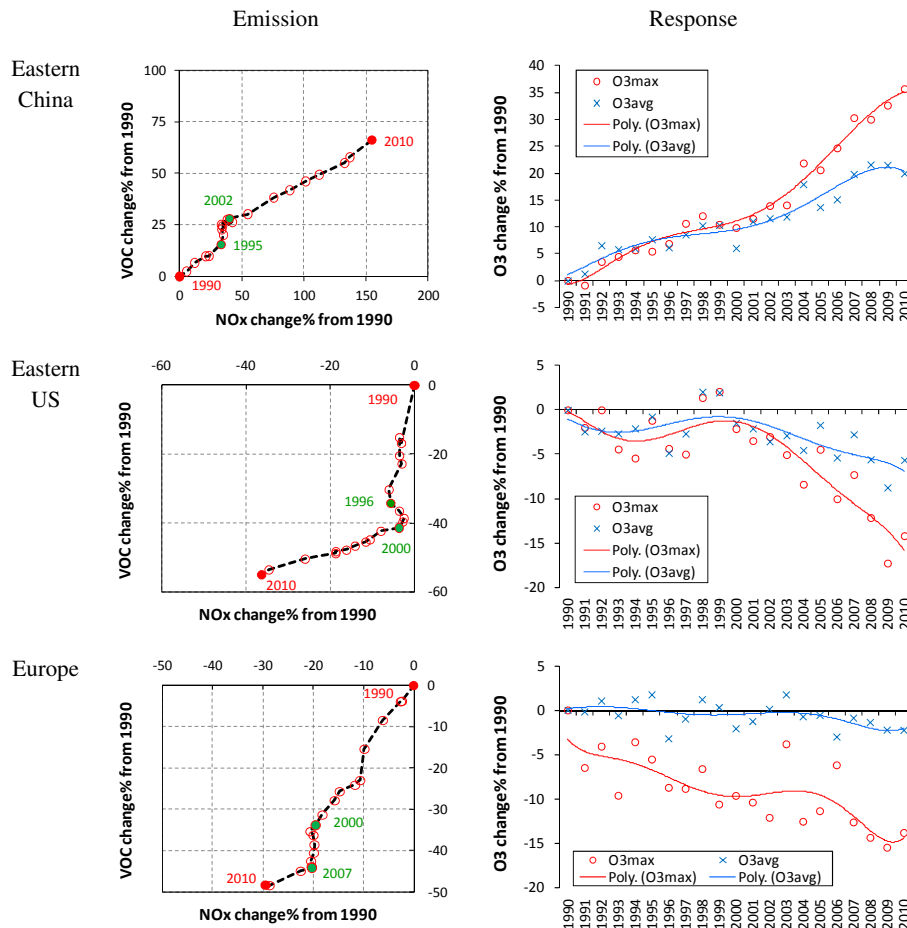


Figure 9. Same as Fig. 3 for EC.

## Observations and modeling of air quality trends over 1990–2010 across the Northern Hemisphere

J. Xing et al.



**Figure 10.** Changes in  $O_3$  chemistry from modeling results (grid-averaged for three regions, O3max – maxima DM8  $O_3$  in each year; O3avg – averaged DM8  $O_3$  in each year; Poly – trend fit by 6th order polynomial regression).

## Observations and modeling of air quality trends over 1990–2010 across the Northern Hemisphere

J. Xing et al.

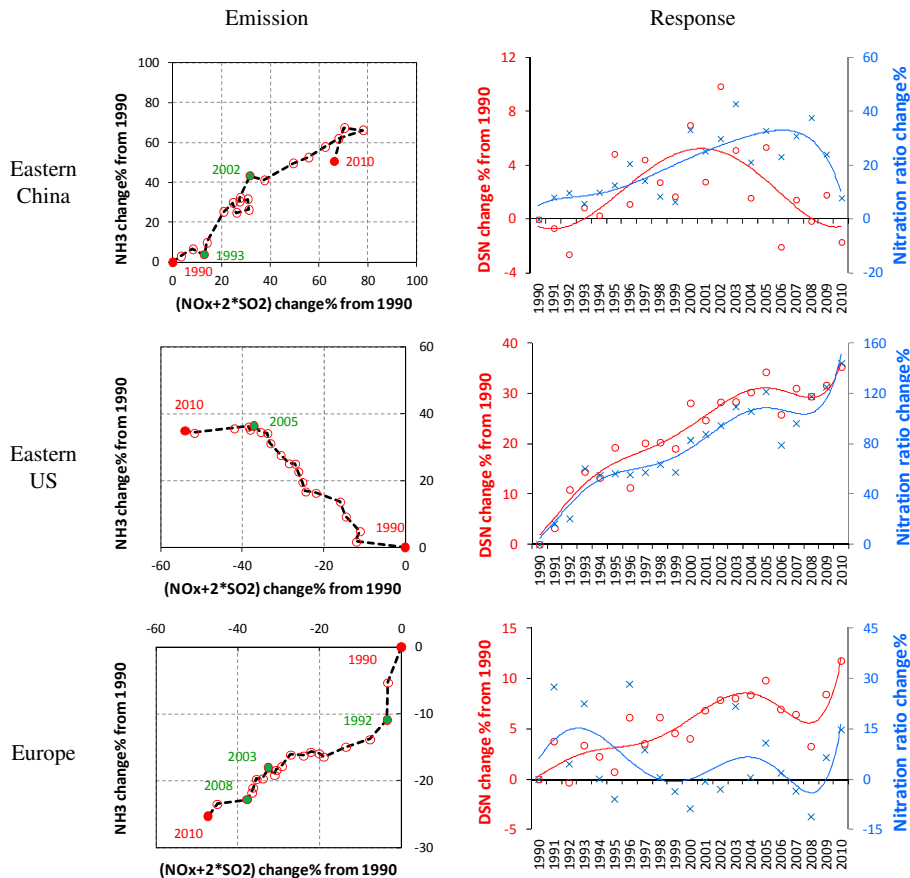


**Figure 11.** Changes in PM chemistry from modeling results (calculation based on molecular units; grid-averaged for three regions;  $(\text{NO}_x + 2 \times \text{SO}_2)$  represents the amount of  $\text{NH}_3$  needed for complete neutralization; DSN – degree of sulfate neutralization; Nitration ratio =  $\text{NO}_3^-$  concentration/ $\text{NO}_x$  emission).